Deutsche Gesellschaft für Technische Zusammenarbeit (GTZ) GmbH

Soil Erosion in Terrace Farming

Destruction of Farming Land Induced by Changes in Land Use in the Haraz Mountains of Yemen

Horst Vogel

Soil Erosion in Terrace Farming

Destruction of Farming Land Induced by Changes in Land Use in the Haraz Mountains of Yemen

Horst Vogel

Eschborn 1992

Published by: Deutsche Gesellschaft für
Technische Zusammenarbeit (GTZ) GmbH,
Postfach 5180, 6236 Eschborn,
Federal Republic of Germany

Translated by: Gregory G. Woods-Schank, 6900 Heidelberg

Printed by: F.-M.-Druck, 6367 Karben

Foreword

When, in the summer of 1984, I was offered the opportunity to spend about 3 months as a guest at a development cooperation project of the Deutsche Gesellschaft für Technische Zusammenarbeit (GTZ) GmbH focusing on soil conservation and afforestation in former North Yemen (Yemen Arab Republic), my sought-after goal of concluding my university studies in geography with an application-oriented graduation thesis (Diplom-Arbeit) had become reality. For this purpose, "soil erosion in terrace farming" presented itself as an exemplary area-oriented and thus geographically relevant topic which would permit me to practically apply what I had learned at university about physical and anthropological geography, while at the same time broadening my knowledge in an extraordinarily fruitful manner.

I would like to extend my heartfelt thanks above all to my counselor, Prof. Dr. H. Kopp of the Geographical Institute of the University of Tübingen, for his time and effort, and to the former project leader, Mr. Reinhard Kastl of the GTZ; both of them contributed significantly to my receiving the chance to work on the project, which imparted to me invaluable experiences both of a personal nature and of relevance for my future professional work. I am also grateful to Mr. Kastl and his wife Theresa for their generous hospitality during my stay in Yemen, which permitted me to concentrate fully on my field studies.

Inspired by what I had learned and seen while working at the project, in 1985 I also accepted an invitation from the "International Soil Conservation Organization" to attend the "IV International Conference on Soil Conservation" in Maracay, Venezuela, which was devoted to the theme of "soil and water conservation to prevent food shortage". At this conference, I presented some of the principal theses of the present paper to an international circle of experts. For the generous financial support granted for my participation at this conference I would like to reiterate my thanks to the Tübinger Universitätsbund.

In addition, I want to thank all of those who helped me write this paper by providing expert advice and/or literature, including some unpublished studies. In particular, I wish to thank:

- Dr. H. Aust of the Bundesanstalt für Geowissenschaften und Rohstoffe (German Federal Agency for Earth Sciences and Raw Materials) in Hanover, Fed. Rep. of Germany.
- Dr. E. Bergsma of the International Institute for Aerospace Survey and Earth Sciences in Enschede, the Netherlands.
- Prof. N. Hudson, author of the classic work "Soil Conservation", in Ampthill, Bedfordshire, England.
- Dr. H. Hurni, leader of the "Soil Conservation Research Project" in Addis Abeba, Ethiopia.
- Mr. G. Koch, Director of Cartography at the Geographical Institute of the University of Tübingen, Fed. Rep. of Germany.
- Prof. Dr. J. Loeschke of the Institute for Geology and Paleontology of the University of Tübingen, Fed. Rep. of Germany.
- Dr. H. Rid, the author of "Das Buch vom Boden", in Munich, Fed. Rep. of Germany.
- Prof. M. Singer of the Department of Land, Air and Water Resources of the University of California at Davis, USA.
- Prof. Dr. M. Williams of the School of Geography in Oxford, England.
- Prof. Dr. W. Weiskirchner (deceased) of the Mineralogical-Petrological Institute of the University of Tübingen, Fed. Rep. of Germany, for preparing the thin rock sections.

Tübingen

March, 1986 Horst Vogel

Table of contents

List of tables

List of maps

List of figures

List of photographs

I. Introduction

1. Terms of reference and methodology

As already mentioned in the foreword, this thesis was written within the scope of a 3-month stay at a project of the Deutsche Gesellschaft für Technische Zusammenarbeit (GTZ) GmbH, a government-owned organization in the Federal Republic of Germany which operates in the field of bilateral technical cooperation projects in countries of the Third World.

The "Haraz-Pilot-Project for Erosion Control & Afforestation" in the Jabal Haraz area of the former Yemen Arab Republic (North Yemen) had just recently completed its 3-year pilot phase when I arrived on the scene to carry out my field studies between August 20 and November 7, 1984. Due to the long previous isolation of North Yemen, basic data related to the problem of soil erosion in this outer tropical mountainous region was hard to come by - for the most part, the only available sources were descriptions of a general nature.

I was thus initially confronted with the task of extracting concrete information on the basis of an area survey. In my opinion, such a survey is an essential prerequisite for implementation of appropriate soil conservation measures and accompanying land-use planning (cf. Hurni 1979, p. 159; Hudson 1981, p. 188; Leser 1983a, p. 18).

Having recognized that the various morphodynamic processes involved in soil erosion can only be understood and combatted if the natural and human factors influencing erosion and their complex interactions are known, I surveyed both the physical mechanisms of apparent relevance to the area under study and the basic geographical and environmental situation.

The foremost objective of this work was both to identify the dynamic processes characterizing the various soil-erosion processes and their dependency on geographical factors, and to map the latter for the entire study area.

I chose which erosion-relevant factors to study on the basis of the soil erosion model advanced by W. WISCHMEIER and D. SMITH (1978):

1. The climate - in particular, rainfall erosivity, the frequency of high-intensity rainfall, and total rainfall.

2. The soils - in particular, soil erodibility.

3. The relief - in particular, the natural relief energy and man-made microrelief.

4. Cultivation - in particular, the land-use practices.

5. Lithology - in particular, the susceptibility of the rocks to weathering.

These soil erosion factors were recorded in the form of tables, diagrams, photographs and maps, and in this form represent a solid basis for assessing the "mean" erosion risk in the study area. In addition, I endeavored to quantify the extent of recent soil erosion and the magnitude of erosive phenomena to be expected in future.

Since narrow limits were imposed on the field work by the available time and equipment, I was forced to make use of simple, for the most part semiqualitative, semiquantitative field methods, most of which I either borrowed from comparable application-oriented studies or devised myself. So that the results obtained would yield the best possible, i.e. representative, picture of soil erosion in the study area, I consistently conducted my field work along the lines of the multiple-stage measurement, mapping and observation methodology developed by the "Basel School" (Fig. 1; Schmidt 1983, p. 54; Leser 1983a, p. 17; G. Richter 1983, p. 38).

Fig. 1: The "Basel multiple-stage measurement method"

DIMENSION	METHODS	OBJECTIVES
SINGLE POINT	● Test plot ● Micro plot ● Rainfall simulation	Collection of basic data on individual factors and soil erosion processes
MEDIUM-SCALE (field measurement)	● Field station ● Field box ● Erosion-measuring stake	Measurement of soil removal under natural field conditions; comparison with single-point measurements
LARGE-SCALE (regional measurements)	● Complex mapping of damage ● Regional soil loss and sediment yield	Type and spatial distribution of soil erosion; soil and nutrient losses from overall area

Source: R.-G. Schmidt (1983, p. 54)

These activities were supplemented by several interviews of local residents towards the end of my stay in the field, carried out with the aid of the project interpreters; these primarily served the purposes of assigning a time frame to abandoned terrace complexes and evaluating perception of the problem on the part of members of the local population.

The preceding comments are intended to point out that soil erosion research, which is essentially a field of earth science, should never lose sight of its real aim, namely to combat soil erosion; in other words, research results should, at the very least, be indirectly of relevance to a practical application (Leser 1983a, p. 213). For the geographer, this implies the necessity of considering not only the qualitative aspects of current relief development and surface layer displacement (e.g. forms, geographical distribution, classification, patterns), but also matters related to the quantitative morphodynamics of the individual processes involved and to the relative magnitudes of soil erosion (soil erosion prognosis) (cf. Leser 1978, p. 49). Only if the causes, dynamics and effects of soil erosion are systematically studied, evaluated using standardized criteria, and if possible quantified, is it possible to shed light on this complex of interacting processes in the interest of controlling soil erosion (cf. Capelle and Lüders 1979, pp. 885-886).

Armed with this understanding of the problem, I carried out a selective theoretical and practical survey of the relevant fundamentals, concentrating the field work on a selected geomorphologically representative study area in the vicinity of the project headquarters. The basic theoretical aspects which are discussed in detail in the first chapters of this paper are intended to characterize the physical-geographical factors which govern an outer tropical mountain region like the Haraz area. This provides the necessary basis for assigning the various soil-erosion processes to specific environmental contexts. Building upon this, well-founded prognostic conclusions can then be derived.

2. Discussion and definition of the concept of "soil erosion"

H. BENNETT (1939), one of the pioneers of modern soil erosion research, considers that soil erosion comprises all accelerated soil removal processes performed by the wind and water, most of which are induced by human activities.

In particular, H. BENNETT makes the following distinctions:

1. Normal, or geologic, erosion
2. Accelerated, or soil, erosion
   a) naturally accelerated erosion
   b) man-induced or artificial erosion

(Bennett 1939, pp. 6, 92-94, 947-950)

As opposed to man-induced soil erosion, naturally accelerated erosion results from impairment of the cover of vegetation caused by severe drought, plant disease, avalanches, etc. (Bennett 1939, p. 948).

H. BENNETT thus regards soil erosion as being the sum of all soil removal phenomena that interfere with the environment and/or the dynamic balance between formation of new soil and soil removal, accelerating soil removal to the point that the ability of affected areas to sustain agriculture on a long-term basis is threatened. From the point of view of the active forces involved in removal and transport of surface soil, he distinguishes between erosion by water (water erosion) and erosion by wind (wind erosion) (Bennett 1939, pp. 949-950; cf. Bargon 1962, p. 480; Semmel 1978, p. 418; Breburda 1983, pp. 13-16).

D. ZACHAR (1982), among others, counters that this equivalence of soil erosion and accelerated soil removal (although many authors confine themselves to anthropogenically induced accelerated soil removal, e.g. Grosse 1971, p. 11; G. Richter 1973, p. 377; Hurni 1975, p. 158; Späth 1976, p. 122; Kugler 1985, p. 123) is unsatisfactory because, for example, in drought-prone regions it is extremely difficult to distinguish between naturally accelerated erosion and the geologic norm of erosion, and moreover the loss of soil from agriculturally utilized land can sometimes be less than the natural rate of soil removal (Zachar 1982, pp. 22-24).

In my opinion, evidence in support of the second objection is provided by the terraces of former North Yemen, which when properly maintained not only largely eliminate the high-natural susceptibility to erosion of these outer tropical mountainous areas, but even permit them to sustain agriculture (since the fields are enlarged and replenished by accumulation of weathered material).

For the sake of simplicity, D. ZACHAR therefore proposes defining the concept of soil erosion as broadly as possible instead of restricting it to soil removal accelerated by human interference or natural events. In his view,

soil erosion can take the form of natural or human-influenced erosive processes, both in geologically normal and abnormal dimensions, and on either an anthropogenically accelerated or reduced sale (Zachar 1982, p. 24). With this broadening of the definition, however, in my opinion D. ZACHAR succeeds in thoroughly distorting the original intention of the term. It was coined in response to the devastating loss of soil in the continually expanded grain-growing areas of the Midwest of the United States, which attracted worldwide attention during the 1930s and the shocking extent of which ultimately led to the establishment of the U.S. Soil Conservation Service under the direction of H. BENNETT.

I therefore believe that the concept of soil erosion should be reserved for erosive processes that lead to impairment of agricultural utilization in the medium term and destruction of the soil in the long term.

In view of the fact that it is not possible to make a clear distinction between anthropogenically and naturally induced soil-erosion processes in naturally delicate mountain ecosystems like that of the Haraz district, for the purposes of this paper I have applied the following definition of soil erosion:

"Soil erosion is a quasi-natural process which is triggered by natural or artificial causes and then naturally continues, although it is then usually again favored by human activities. In most cases, however, it is both anthropogenically induced and promoted" (Leser 1983, p. 15).

II. The role of soil erosion in functional geoecosystems

1. The factors involved in water erosion according to the "Universal Soil Loss Equation" of W. WISCHMEIER and D. SMITH

The processes involved in soil erosion are the visible expression and result of a long-term disturbance of the complex of interacting forces associated with the land and its environment, as a consequence of which the natural dynamic equilibrium between those forces which are conducive to erosion (erosive forces) and those which inhibit erosion (resistive forces) is decisively tipped in favor of the erosive factors.

This shift has attracted the interest of human beings not because they are responsible for having caused it - which they usually are - but rather because the soil erosion dynamics thus set in motion threaten their survival by gradually destroying the fundamental agricultural resource represented by the soil. Any attempt to ward off this threat to our existence by implementing effective conservation measures must be based on an understanding of the factors involved.

In the case of water erosion, these factors were first systematically treated in the soil erosion model developed by W. WISCHMEIER and D. SMITH (1978), namely the "Universal Soil Loss Equation" (USLE). According to this model, the actual extent of soil erosion - i.e. induced by human occupation and land use - is determined by the interaction of the following factors:

1. The erosive forces of the rainfall and associated runoff
2. The susceptibility of the soils to erosion
3. The morphology of the land slope
4. Land use (vegetal cover)
   a) Soil and crop management systems
   b) Conservation practices

(Wischmeier 1977a, p. 45; Wischmeier and Smith 1978, p. 4)

Although some of the diverse interactions and complicated feedback mechanisms among the various factors are still in need of definitive analysis, it is nevertheless possible to identify direct connections between the individual factors and the overall phenomenon, or in other words, the potential and/or current risk of erosion. While the potential risk of erosion (inherent erosion potential) of a site results from the combined effect of the factors of climate, soil and relief, the current (effective) risk of erosion is also influenced by human activities. These can either have an inhibiting effect (thus reducing the inherent natural risk of erosion) or an aggravating effect (i.e. inducing soil erosion).

2. The "Universal Soil Loss Equation", its predictive power and applications

The "Universal Soil Loss Equation" (USLE) is, for the time being, the last of a series of equations for calculating soil erosion which have been developed in the United States since the early 1940s.

These efforts began with an empirical erosion formula advanced by A. ZINGG, which expressed the measurable soil loss as a function of the steepness and length of the land slope (single-factor equation) (Kent Mitchell and Bubenzer 1980, pp. 17-22; Morgan 1979, p. 51; Hudson 1981, p. 193).

As researchers learned more about soil erosion and more experimental erosion data became available, one after the other all of the factors influencing the process of water erosion were gradually included in such equations (multiple-factor equations), although these initially yielded usable results only for relatively small areas. It was not until the USLE was developed by W. WISCHMEIER and D. SMITH (1960; 1978) that it became possible to assess larger areas. During the years that followed, this model was successfully applied to increasingly large land areas in the United States (Wischmeier and Smith 1960, p. 418; 1978, pp. 1-2).

This development was made possible by an immense body of runoff and erosion data obtained from standardized test plots and non-standardized control plots, and statistically analyzed with the aid of computers. Evaluation of this extensive catalog of basic data revealed that the long-term mean annual soil loss from individual plots (fields, slope sections) can be adequately explained and approximately quantified using a total of six different variables. Thus:

$$A = R \times K \times LS \times C \times P$$

where:

- A = mean long-term soil loss
- R = rainfall and runoff erosivity factor
- K = soil-erodibility factor
- LS = topographic factor
  - slope length factor (L)
  - slope steepness factor (S)
- C = cropping and management factor
- P = erosion-control factor

(Wischmeier and Smith 1960, pp. 419-20; 1978, p. 4; cf. Scheffer and Schachtschabel 1982, pp. 422-423; Arbeitsgruppe Bodenkunde 1982, p. 171)

The most important parameters for the USLE are the R and K factors. R is the rainfall and runoff erosivity factor, and unless the erosivity is increased by runoff from thaw, snowmelt or irrigation, it equals the total average annual erosive energy of the rainfall and its associated runoff, expressed in so-called rainfall-erosivity units (EI). K is the soil-specific susceptibility to erosion (erodibility expressed in units of weight per units of area for each rainfall-erosivity unit (EI the units used to express R).

The basic form of the Universal Soil Loss Equation is therefore :

$$A = R \times K$$

This basic formula was established with the aid of soil loss measurements performed on standardized test plots having a uniform length of 22.13 m (72.6 ft) and a uniform width of 1.83 m (6 ft), as well as a constant slope steepness of 9%. The plots were also subject to full fallow, i.e. at the time of the tests they had been kept free of vegetation for more than two years, and tilled parallel to the direction of the land slope. The soil removal rates attained their potentially highest values on these standard plots, as a function of the erosive force (kinetic energy) of the rainfall and associated surface runoff, and of the inertial force or resistance of the soil.

Parallel to this, soil loss measurements were performed on plots with different slope topographies and land-use patterns, both with and without application of supplementary soil conservation measures. The data thus collected was also statistically analyzed, and used to determine the relative influences of differing slope topography (LS factor), plant cover and management practices

(C factor), and implemented soil conservation practices (P factor). Under site conditions identical to those on the standardized test plots, these dimensionless factors are all assigned the value of 1, while the soil loss rates measured on the standard slope must be adjusted upward or downward to take real relief and land-use conditions into account (Wischmeier 1977a, Wischmeier and Smith 1960; 1978).

Finally, all of the erosion factors used in the USLE were depicted in maps, tables and nomographs from which the values of the factors could be either directly read or derived by applying appropriate techniques. In this form, they serve the principle purpose for which the USLE was devised, namely to provide soil conservation planners and field technicians with a readily available and dependable working tool for systematic elaboration of effective soil conservation practices (Wischmeier 1977b, p. 371; Wischmeier and Smith 1978, pp. 3 and 40). First, however, the maximum permissible soil loss rate (soil loss tolerance or T value) must be identified, and the potential erosion risk calculated by multiplying together the R, K and LS factors. The product of these three factors yields the highest possible average long-term soil loss on the studied plot for full fallow when C = 1 and P = 1.

In order to ensure sustained use of a studied plot while preserving soil fertility and soil mass, the management practices and any required soil conservation measures must be chosen in such a way that, at the very least, the condition A = T is met. In the method advanced by W. WISCHMEIER and D. SMITH (1978), this aim is achieved by dividing T by A to determine the highest possible value for the C factor (cover and soil management). The value thus obtained for this factor is then checked against the working tables compiled for the C factor, which gives consideration to the individual developmental phases (crop stages) of the crops for a large number of different combinations of crop rotation and cultivation methods (Wischmeier and Smith 1978, pp. 17-34). On the basis of the factor assignments listed in these tables, concrete management practices can then be proposed for each individual plot. If supplementary erosion control measures are practiced, then the highest possible value for C is increased by the factor 1/P. In this case, the equation is:

$$C \times P = T / (R \times K \times LS)$$

This relation of course also holds for cases in which conservation methods must be implemented because none of the management methods listed in the working tables fulfill the condition A = T (Wischmeier 1977b, p. 373; Wischmeier and Smith 1978, pp. 42-44).

In an initial state of euphoria over the diverse possibilities for practical application of the USLE and its relative ease of use, many let themselves be lured into employing it for tasks for which it had not been intended or in regions for which no factor values had yet been compiled (cf. Hudson 1981, p. 201).

The real objective pursued with the USLE is determination of average long-term soil loss from individual plots in order to permit, once the site soil loss tolerance has been established, elaboration of effective soil conservation methods for them in the form of appropriate management systems and, if required, erosion control measures (Wischmeier 1977a, p. 45; 1977b, p. 371; Wischmeier and Smith 1960, p. 423; 1978, pp. 2-3).

It does not provide, however, any reliable predictions on the extent of soil erosion in any given year or, much less, that caused by individual rainfall events; nor is it suited for assessing the soil loss of entire drainage basins, since the slope topography factor LS, among other things cannot be applied to such large areas. One consequence of this restriction is that (intermediate) sediment accretions at the toe of field slopes, along field boundaries, and in channels, waterways and runoff paths are not taken into account (Wischmeier 1977b, pp. 371 and 374; Wischmeier and Smith 1978, pp. 45-46).

A further important limitation is due to the often overlooked fact that the concepts of soil erosion, erosivity and erodibility are very narrowly defined in the USLE. Thus, this erosion formula considers only the erosional processes typical of farming tracts (i.e. sheet, splash and rill erosion), but excluding gully erosion and the parameters which govern it (Hudson 1980, p. 282). If gully erosion is active in a study area, then the soil loss values computed with the aid of the USLE must be adjusted upward by the soil loss caused by gullying in order to obtain a realistic idea of total soil loss (gross erosion) (Wischmeier and Smith 1978, p. 46).

In addition to these practical and thematic limitations, the character of the USLE as regards data collection techniques also poses questions and problems of a fundamental sort. Since all of the relations worked into this so-called "*Universal* Soil Loss Equation" are of an empirical nature, strictly speaking they reflect only the site conditions where the experimental studies on which it is based were performed, i.e. the climatic, soil, relief and land-use conditions typical of the eastern part of the United States (without the eleven mountain states in the West) (Stocking 1978, p. 142; Hudson 1980, p. 280; Leser 1983a, p. 215).

Consequently, when the factorial relations identified by W. WISCHMEIER and D. SMITH (1978) are transferred to site conditions other than those on which the USLE was based, the more these differ the greater is the risk of extrapolation errors, especially where the slope topography factor LS is concerned (Wischmeier 1977b, p. 376). The accuracy of the soil loss values computed with the aid of the USLE, which in no way can be regarded as more than the best possible approximations, is therefore greatest when studying tracts with a slope percentage of between 3 and 18% and a slope length of less than 122 m (400 ft), and the soils of which exhibit a uniform particle distribution comparable to that of loessal and morainal landscapes (Schwertmann 1981, p. 20). Moreover, the land-use systems and management methods of the studied area should be comparable to those of capital-intensive, highly mechanized agriculture in the United States, and the erosivity must be determined by rainfall structures like those characteristic of the temperate latitudes (Wischmeier 1977b, pp. 372-373 and 376; Wischmeier and Smith 1978, p. 49).

Because of all these geographical and thematic constraints on application of the USLE, the internationally renowned soil erosion expert N. HUDSON (1980, p. 279) regards the designation "universal" as being probably the "most unsuitable name" conceivable. Even W. WISCHMEIER (1977b) himself felt obliged to warn against misuse of the USLE in a separate paper and to once again clarify the purpose for which it was intended and the applications for which it is suited.

Meaningful transfer of the USLE to landscapes in other parts of the earth is possible only following prior experimental checks and, if necessary, reevaluation (adaptation) of the component factors and/or factorial relations. This approach was used, for example, by a working group headed by U. SCHWERTMANN (1982) in Bavaria; the results of this group's research were also applied to other parts of the Federal Republic of Germany (Arbeitsgruppe Bodenkunde 1982). A greatly simplified procedure was chosen by the FAO et al. (1979) for Africa north of the equator and the Near East. In North Yemen in Chapter V of this paper, I present the estimated values listed by the cited study for the current and potential risk of soil erosion.

The outstanding achievement of the soil erosion model of the "Universal Soil Loss Equation" (USLE) developed by W. WISCHMEIER and D. SMITH (1978) is that, for the first time, it allows all detectable geoecofactors having an influence on erosion to be systematically compiled and their interactions quantified. At least in the United States, where extensive and detailed studies

were carried out to determine the roles of the various factors, realistic quantification of site erosion risk is now possible (Stocking 1978, p. 144; Kent Mitchell and Bubenzer 1980, p. 56).

Where these conditions are not fulfilled - as is the case in nearly all of the developing countries - this model, due to its highly logical structure, can nevertheless be applied as a methodological aid and framework for study and capture of erosive factors (cf. Hudson 1981, p. 204). As such, it was also applied within the scope of the work for this paper in conjunction with the measurement, site surveying and mapping methods described further below.

3. The physical mechanisms of water erosion

a) The physics of water erosion

Planning and implementation of effective soil conservation and erosion control measures must start with thorough knowledge of the dynamics of soil erosion and thus, ultimately, of the various factors which influence erosion. The latter must be derived from the physical mechanisms involved in erosion (Schwertmann 1982, p. 10).

In the case of water erosion, it is necessary to distinguish between the effects of rainfall (the impact and splash effects of falling raindrops) on the one hand and the effects of flowing water (dislodgement and transport of soil by surface runoff) on the other hand. Although basically distinct from one another, these two erosive processes share the fact that, regarded from the point of view of physics, they represent the result of work performed by kinetic energy (Hudson 1981, p. 64; Breburda 1983, p. 42).

The energy sources are the falling raindrops (impact energy) and the flowing water (flow energy). The work performed by rainfall and surface runoff as a result of their motion (induced by gravity) is functionally dependent on the velocity and mass of the water in motion.

Basically, the following general equation holds for the kinetic energy of bodies that, like falling raindrops and flowing water, only describe a progressive (unidirectional) motion.

$$E_{kin} = m/2 \times v^2$$

where:

E_{kin} = kinetic energy
- impact energy
- flow energy

m = mass
- rainfall
- runoff

v = velocity
- impact velocity
- flow rate

(Cooke and Doornkamp 1974, p. 28; Hudson 1981, p. 61; Breburda 1983, p. 42)

This energy is used up by dislodgement or detachment of soil particles from the surface (erosion proper) and their lateral displacement (transport). As soon as the kinetic energy of the impacting raindrops and the surface runoff has been exhausted, the transported soil particles are deposited (colluvial sedimentation).

From the relationship expressed in the energy formula above, it is apparent that the kinetic energy of the moving water increases proportionally to the product of its mass and the square of the velocity; in other words, the energy available for causing soil erosion (dislodgement plus displacement) depends to a much greater extent on the impact velocity and/or rate of flow than on the (effective) quantity of rainfall or runoff.

In the final analysis, the amount of kinetic energy actually carried by the falling raindrops and that portion of the rainwater which flows off as surface runoff depends on the energy-related attributes of the site-specific erosive factors (e.g. rainfall intensity, slope steepness, plant cover, water infiltration capacity of the soil) (Breburda 1983, p. 42).

b) Rainfall erosivity and means of calculating it

The impact of rainfall plays an important role within the context of the dynamics of water erosion. Although its importance was recognized by the pioneers of soil erosion research, in other words as early as the 1930s, gaps still remain today in our knowledge of the factors involved and their interactions (cf. Bryan 1977, p. 67).

Research on this topic was prompted by the observation that the amount of material in suspension in surface runoff rapidly grows with increasing kinetic energy of the falling raindrops (Cooke and Doornkamp 1974, p. 27; Thornes 1979, p. 260). In the course of the experimental studies subsequently performed, the process of raindrop impact was revealed to play a central role within the overall process of soil erosion by water, comprising its actual initial stage (Hudson 1981, p. 39).

When falling raindrops strike bare ground, soil granules and clods are shattered by the force of the impact (drop impact), and the finer particles are separated (detached) by being hurled into the air in all directions (splash effect). This process is referred to as splash erosion (Wischmeier 1977a, p. 47; Hudson 1981, p. 64). In terms of physics, what actually happens is that the kinetic energy of the falling raindrops is transformed upon impact into pressure and into the kinetic energy of loose soil particles (Breburda 1983, p. 45).

The effects of splash erosion are particularly devastating on structurally unstable, recently tilled soils, the granules and small clods of which represent ideal "targets" for the falling raindrops, being rapidly disintegrated and converted into mud by them (cf. Gehrenkemper 1981, p. 50). However, splash erosion by itself is only possible if the falling rainwater is immediately and completely absorbed by the soil or if the placement of the site with respect to the surrounding relief permits little or no surface runoff (Evans 1980, p. 121; Breburda 1983, p. 46).

If the rainfall intensity exceeds the rate at which the water is absorbed by the soil, then so-called thin sheet flow of the "Horton overland flow" type develops (Derbyshire et al. 1979, p. 53), the primary action of which is to wash soil particles downhill which are already detached or have been freed by the impact of the raindrops. This process is referred to as sheet erosion. On gentle slopes the detachment capability of sheet erosion is also determined by the impact energy of the raindrops and is directly proportional to the kinetic energy of the raindrops (Wischmeier 1977a, p. 47; Roose 1980, p. 154; Morgan et al. 1982, p. 71).

In order to assess soil loss caused by splash and sheet erosion, therefore, detailed information on the energy of the rainfall is needed. Since comparisons of energy values computed with the aid of various equations applied to actual soil loss measured on test plots revealed that the total energy of the rain cannot be directly correlated with the amount of soil loss,

it was necessary to develop empirical indices for practical soil erosion studies that are aimed at measuring the erosive force, i.e. the *erosivity* of rainfall.

The two most important and widely used systems are the EI_{30} index developed by W. WISCHMEIER and D. SMITH (1960; 1978) and the KE25 index elaborated by N. HUDSON (1981). They involve quite similar calculations, since they are both based on empirical energy formulas that make use of the following relation between the kinetic energy of rainfall and rainfall intensity:

Under the influence of gravity, the fall velocity of free-falling raindrops increases with drop size (mass). The largest drops attain a maximum diameter of approx. 5 to 6 mm and a maximum impact or terminal velocity of about 9 m/s (Stocking and Elwell 1976, p. 10; Hudson 1981, pp. 53-56). Studies conducted in the United States and Zimbabwe have shown that the median drop size increases with intensity up to a threshold value of 76 mm/h (Wischmeier and Smith 1978, p. 5) and the modal value of the median drop size, i.e. the most frequent and largest median drop size for a given intensity, increases with intensity up to levels of between roughly 80 and 100 mm/h (Hudson 1981, pp. 53-54). At greater rainfall intensities no further increases can be observed; rather, there is even a tendency for the predominantly largest median drop size to decrease (Wischmeier and Smith 1978, p. 5; Hudson 1981, pp. 54-55). This implies that the kinetic energy per mm of rain remains constant at higher intensities (Wischmeier and Smith 1978, p. 56) or exhibits only minimal additional increases (Hudson 1981, pp. 58 and 70) (see Fig. 2).

W. WISCHMEIER and D. SMITH (1978, p. 56) express this relation between rainfall energy and rainfall intensity with the following empirical equation:

$$E = 210 + 89 \log I$$

where:
E = kinetic energy in t/ha per cm of rainfall
I = intensity in cm/h (max. 7.6)

or

$$E = 11.9 + 8.7 \log I$$

where:
E = kinetic energy in J/m^2 per mm of rainfall
I = intensity in mm/h (max. 76)

(Hudson 1981, p. 59)

N. HUDSON (1981, pp. 59 and 71) calculates the kinetic energy per mm of rainfall as a function of rain intensity with the aid of the following formula:

$$E = 30 - 125/I$$

where:
E = $J/m^2/mm$
I = mm/h

From this, it is evident that the *kinetic energy of rainfall* is a function of *rainfall intensity* and *total rainfall*.

If recording rain-gage data is available for determining these two parameters, the erosive potential of a rainstorm can be calculated with the aid of these two empirical formulas or obtained by consulting a chart - as a function of mm of rainfall (Fig. 2).

Fig. 2: Relation between kinetic energy and intensity of rainfall (acc. to Hudson as measured in Zimbabwe, and Wischmeier and measured in the United States).

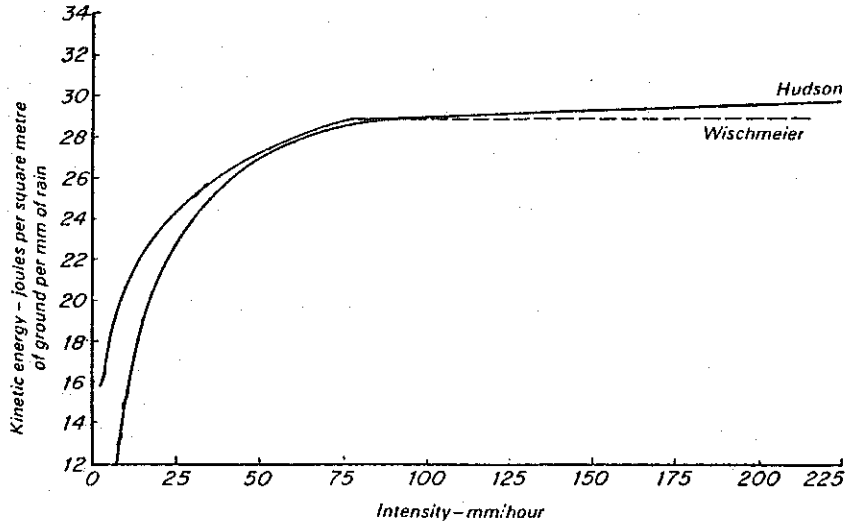

Source: adapted from Hudson (1981, p. 58)

From a practical point of view, however, this is the limit of what these two systems have in common, since they then take diverging approaches to assessing the erosive potential of rainfall (erosivity).

For instance, evaluations of extensive data collected in the United States showed that there is a linear relation between soil loss at the studied sites and a rainfall-erosivity index which is referred to as the EI_{30} index. This index is defined as the product of the total kinetic energy of a rainstorm (E x mm of rainfall / 100)[1] and its maximum 30-minute intensity (I_{30}). The annual erosivity index can be obtained by summing the individual storm values, and their average taken over a period of years (20-25 years) (Wischmeier 1977b, p. 373) represents the rainfall-erosivity index EI_{30} for a particular location. This corresponds to the rainfall and runoff factor R used in the USLE, provided that the site-specific erosivity is not increased by water from snowmelt, thaw or irrigation (Wischmeier 1977a, pp. 49-51; Wischmeier and Smith 1978, pp. 5-8).

By comparison, the soil loss measurement carried out by N. HUDSON (1981, pp. 69-74) in Zimbabwe showed that soil loss, which is dependent on rainfall structure, can be more dependably assessed with the aid of an erosivity index which only takes into account the kinetic energy of rainfall in excess of a threshold intensity of *25 mm/h*. The reason is that, in the course of his measurements, it emerged that this threshold value separates erosive from non-erosive rainfall, i.e. soil removal only occurs if a certain minimum rainfall intensity is attained. Accordingly, he calculates rainfall erosivity with the aid of the so-called KE25 index, the value of which represents the total kinetic energy of all rainfall which exceeds the mentioned intensity threshold of 25 mm/h.

The differences between the two erosivity indexing systems presented here are a visible expression of the empirical character of both methods. Since the two indices cannot be exchanged for one another, because of the different calculation procedures used and the inclusion of the additional empirical factor I_{30} in the EI_{30} index, whenever studies are carried out in situations where no body of test data collected over a number of years is available it is always necessary to decide which of these two systems is best suited for assessing the erosivity in a given study area (cf. Hudson 1977,

1) The division by 100 is performed in order to make dealing with the otherwise very large figures easier (Wischmeier and Smith 1978, pp. 6 and 56).

p. 174). Rainfall in outer tropical areas like Zimbabwe can certainly be expected to exhibit different attributes with respect to frequency, duration, intensity and amount as compared with rainfall in the studied areas of the United States, which belong to the temperate zones of the earth.

Taking the example of the KE25 index, which was also used in this study, I would like to expressly point out once again the often overlooked or ignored fact that the concept of erosivity as used in the works of W. WISCHMEIER and N. HUDSON only possesses validity for certain erosive processes and the complex of interacting site factors governing these (Hudson 1980, p. 280). Under the site conditions chosen by both authors, the detachment of transportable soil particles from the ground surface occurs nearly exclusively due to the impact energy of the raindrops, while the associated surface runoff primarily functions as a transport medium (Hudson 1981, p. 75; cf. Roose 1980, p. 154).

N. HUDSON (1981, pp. 71-74), for example, carried out his soil loss measurements in Zimbabwe on test plots having a uniform slope steepness of only 5% and varying field sizes of 1 x 0.3 m and 26.5 x 1.5 m, as well as with the aid of so-called "Ellison-type splash cups". These are measuring cylinders used to capture the soil loss caused by splash erosion alone. In all three two-year test series a high correlation was established between soil loss and the rainfall-erosivity index KE25. Correlation coefficients of 0.92 and 0.94 were obtained for the two differently-sized test plots, respectively, as compared with a correlation factor of 0.96 for the Ellison-type splash cups. This high correlation allows the conclusion to be drawn that most of the soil carried off the test plots by thin sheet flow was also detached by the impacting raindrops, and only to a negligible extent by the flowing water (Hudson 1981, p. 65; cf. Jansson 1982, p. 3).

With a view to application-oriented soil erosion studies, this conclusion implies that the erosivity index of N. HUDSON is suited for evaluating the detachment potential of high-intensity tropical rainstorms (cf. Morgan et al. 1982, p. 73), and is therefore a good choice for applications in development cooperation projects aimed at relatively quick data availability.

However, because of the site conditions under which it was tested, this index cannot be used to assess the risk of gully erosion in a given area (cf. Hudson 1980, p. 280).

To sum up, it can be ascertained that in areas where most of the rain is high in intensity - like in the outer tropics - heavy rains possess an immense amount of kinetic energy and thus correspondingly high erosivity.

c) The tractive force and carrying capacity of surface runoff

In general, surface runoff can arise in two different ways.

According to the classical model of R. HORTON (1945)[2], surface runoff occurs when the rainfall intensity (mm/h) exceeds the infiltration rate (mm/h) of a particular soil. The resulting sheet flow is particularly typical of short, heavy rains in semiarid climatic zones characterized by a sparse plant cover.

In wetter regions, by contrast, maximum infiltration is generally greater than effective rainfall. Without a doubt, vegetation plays a decisive role here (dissipating rainfall energy by intercepting the falling raindrops, and enhancing infiltration). During prolonged rainfall, however, soil moisture can be increased to past the saturation point. The surface runoff thus induced is referred to as "*saturation overland flow*" to distinguish it from "*Horton overland flow*" (Kirkby 1969, p. 219; Derbyshire et al. 1979, p. 57).

Independent of existing cavities and depressions, with increasing slope steepness and length and as a result of cohesion and friction effects, in both cases the initial sheet flows tend to gradually concentrate in a downslope direction into linear runoff channels (Derbyshire et al. 1979, p. 51; Kugler 1985, p. 123).

The kinetic energy of the runoff is usually too low to detach soil particles from the ground surface. Consequently, for the most part the shallow, slowly moving sheet flows only carry very fine, light particles (soil colloids) that are already loose or have been dislodged by falling raindrops (Breburda 1983, pp. 46-47; cf. Evans 1980, p. 115). With highly turbulent runoff and as greater quantities of water collect in branched and parallel runoff channels, however, soil particles are increasingly detached from the ground surface by the shearing action of the flowing water (Wischmeier 1977a, p. 49; Bryan 1977, p. 66; Morgan et al. 1982, p. 71).

The erosive power (detachment capability) of flowing water is expressed as *tractive force*, which is computed with the aid of the DuBoys formula in units

2) Cited in Kirkby 1969, pp. 217-218; Cooke and Doornkamp 1974, pp. 31-38; Thornes 1979, pp. 262-264; Derbyshire et al. 1979, pp. 53-57.

of weight (kg) per unit area (m^2) (Hjulström 1935, p. 292; Strele 1950, p. 47, Cooke and Doornkamp 1974, p. 33; Thornes 1979, p. 263; cf. Breburda 1983, pp. 32 and 43).

In its simplest form the formula for tractive force is as follows:

$$S = G \times T \times J \text{ kg/m}^2$$

where:

S = tractive force in kg/m^2
G = weight of 1 m^3 of water
T = water depth in m
J = slope angle of the water surface in m/m

(Strele 1950, pp. 47 and 37)

Taking into account the specific gravity of water, which attains its maximum density of 1 g/cm^3 at 4°C, the formula for tractive force can be expressed as follows:

$$S = 1000 \times T \times J \text{ kg/m}^2$$

(Späth 1976 p. 127)

If J is substituted from the Chezy formula (Späth 1976, p. 128; cf. Strele 1950, p. 38; Hudson 1981, p. 132) for calculating the mean runoff velocity (V), namely:

$$V = c\sqrt{R \times J} \text{ m/sec}$$

and the hydraulic radius R replaced by the average water depth T (cf. Thornes 1979, p. 262; Derbyshire et al. 1979, p. 54), then one obtains:

$$S = 1000/c^2 \times v^2$$

where:

c = coefficient of roughness

It clearly follows from both the formula for tractive force and the general energy formula already presented that the erosive potential (shearing ability) of flowing water is proportional to the square of the runoff velocity. This in turn, as shown by the Chezy formula, is a function of slope steepness, the depth of the flowing water and the surface microrelief.

According to the velocity formula, if slope steepness is quadrupled, this results in a doubling of the runoff velocity. If the rate of flow is doubled, the

tractive force of the water is quadrupled. At the same time, the *carrying capacity* (quantity of transported soil) of the runoff is increased thirty-two-fold, and the water can carry particles sixty-four times the size of those carried previously (Morgan 1979, pp. 8-9; Zachar 1982, pp. 221 and 281; Breburda 1983, p. 31).

From these fundamental considerations, it follows that the tractive force increases proportionately to the slope steepness. At the same time, there is even an exponential relation between the steepness of the land slope and the potential carrying capacity of runoff. With increasing slope steepness, the possible rate of soil removal is therefore many times greater than the already steadily growing potential detachment rate. Whereas the tractive force (detachment capacity) varies as the square of the rate of flow, the transporting capacity of the runoff increases proportionally to the 5th power of the runoff velocity, and the maximum transportable particle size even to the 6th power.

These facts are of enormous importance for understanding the erosional process, since all other actions contributing additionally to the dislodgement of soil particles (e.g. trampling by livestock, sloughing off of soil by alternate freezing and thawing, the impact of raindrops) appreciably boosts the potential soil removal rate. The impact of falling raindrops plays a major role in tropical regions characterized by very high-intensity rainfalls (impact and splash effect) (Zachar 1982, pp. 221 and 281; cf. Hudson 1981, p. 196).

This confirms that, particularly in outer tropical mountainous areas like the Haraz area, the inherent natural risk of erosion due to the predominant high-intensity rains (high erosivity), the high relief ratio (high tractive force and carrying capacity) and the generally only sparse vegetal cover (providing little stabilization) is very high.

Of great importance for understanding the erosional process is also the fact that the erosive power of the runoff is further raised by the load of particles carried by it, since the abrasive action of the transported material has the effect of detaching additional transportable particles (Wischmeier 1977a, p. 47; Breburda 1983, p. 43; Jätzold et al. 1984, p. 217; Kugler 1985, pp. 112-115).

With increasing sediment content (due to internal friction), however, the runoff velocity gradually diminishes - total runoff, surface microrelief (external friction) and slope steepness remaining unchanged - which expresses itself in a reduction of the runoff energy (Strele 1950, p. 49; Kugler 1985, p. 115). The energy available for detachment of additional soil particles thus also

rapidly diminishes (tractive force), until no further material can be dislodged and carried away. In such a case, the runoff has reached its maximum possible carrying capacity for a given volume of flowing water and runoff velocity, i.e. the available energy is completely expended by transport of the sediment (highest possible rate of soil removal). If additional material is then provided by accompanying erosive processes (e.g. landslides, discharged by tributary flowing waters) or as a result of slope flattening (e.g. at the toe of slopes, or at the base of the wall of a terrace) or as a result of reduced water volume (e.g. caused by infiltration or spreading of the water over a larger area following overflow past a terrace wall), then deposition of sediment (accumulation) begins in the third and final phase of the soil removal process (Breburda 1983, pp. 42-44; Jätzold et al. 1984, p. 217).

The curves compiled by F. HJULSTRÖM (1935, pp. 284) on the basis of experimental data on erosion velocity and sedimentation velocity (lowest

Fig. 3: Relation between flow velocity (cm/s) and erosion, transport and sedimentation of different particle sizes.

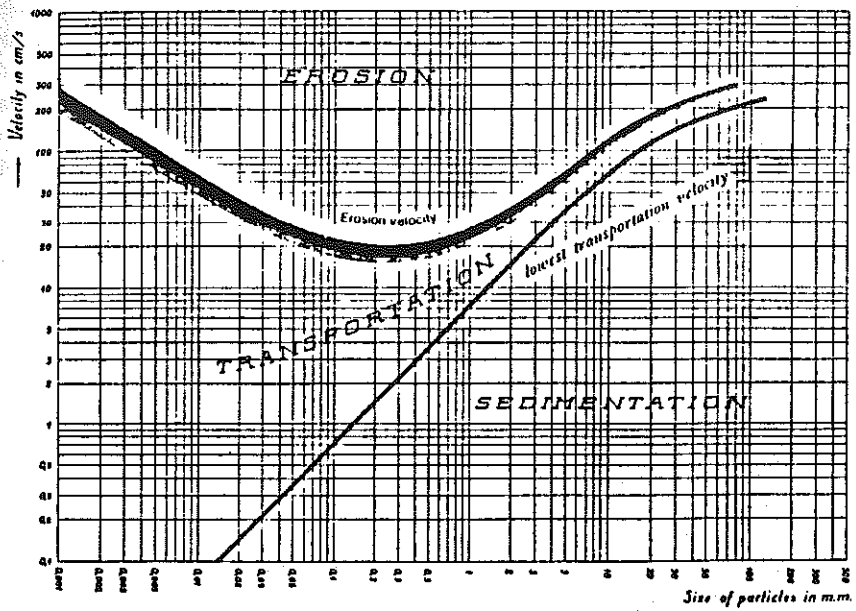

Source: Hjulström (1935, p. 298); supplemented

transportation/settling velocity) permit very convenient determination of the runoff velocities at which different particle sizes are eroded, transported and deposited (see Fig. 3).

According to these studies, the fraction most susceptible to erosion is that comprising coarse silt and sand (0.02-2 mm in diameter), while the clay fraction is quite resistant to erosion due to the appreciable cohesive and adhesive forces acting among the particles (Hjulström 1935, p. 299; cf. Breburda 1983, p. 43). It can also be seen in this chart that detachment of the particles most susceptible to erosion (0.1-0.5 mm in diameter) sets in at a critical erosion velocity of approx. 16 to 18 cm/s. According to T. DUNNE (1978, cited in Derbyshire et al. 1979, pp. 54 and 58), such velocities are rarely attained by sheet flow, which typically moves at a rate of between 0.3 and 15 cm/s (cf. Breburda 1983, p. 47). Significant entrainment of soil particles by flowing water can therefore only be expected along runoff channels in which water collects, e.g. in the case of stream-like runoff (gully erosion). The same also holds for transport of larger particle sizes (pebbles, rocks) (see Fig. 3; cf. Kugler 1985, p. 123).

When splash and sheet erosion occur concurrently, which is the case with prolonged rainfall and slow-moving surface runoff, considerable turbulence is caused by raindrops impacting on the shallow flow, thus leading to increased detachment of soil particles and an appreciably greater transporting capacity (Wischmeier 1977a, p. 47; Evans 1980, p. 115; Hudson 1981, pp. 65-66; Breburda 1983, pp. 44-46). Under such conditions, the high kinetic energy of the falling raindrops is directly expended for detachment of particles or converted into kinetic energy of the surface runoff.

Comparable erosion-enhancing turbulence of flowing water is also caused by eddy formation around rocks and plants, by pulsating runoff as a result of microdamming, and above all by eddy and roll formation where the water spills over steep drops in the slope (e.g. at terrace walls) (Strele 1950, p. 45; Bryan 1977, p. 66; Jätzold et al. 1984, p. 216).

To sum up, it can be concluded that two threshold values for the runoff velocity exist for a given particle size, namely a higher value for entrainment (erosion velocity) and a lower one for deposition (sedimentation velocity). These are the visible expression of the various exponential relations demonstrated above between runoff velocity on the one hand and tractive force and carrying capacity on the other.

Strictly speaking, the values shown in Fig. 3 apply only to channels at least 1 m deep with a bed consisting of loose material with a uniform particle size

distribution (Hjulström 1935, pp. 294-296). Since, however, soil in reality exhibits a heterogeneous particle size distribution, with the finer particles being protected by the coarser ones, the actual erosion rates deviate somewhat from those indicated in Fig. 3 (Hjulström 1935, p. 300), although this protective effect is offset by high runoff turbulence caused by impacting raindrops and/or frequent steep drops in the slope.

This implies that under environmental conditions characterized by such influences - like those of the abandoned terrace complexes in the Haraz mountains - even thin sheet flows can cause considerable soil removal.

4. The central factors of relief and vegetation

As the above discussion of the factors influencing the dynamics of soil erosion has shown, water erosion is strongly governed by the land relief. Although the DuBoys and Chezy formulas and the Hjulström curves were developed for channels, they also apply in principle to soil-erosion processes of the sheet flow type. In shallow sheet flows, however, the erosive energy is considerably less than in channeled runoff paths (Cooke and Doornkamp 1974, pp. 31-34; Späth 1976, p. 128; Kugler 1985, p. 123; cf. Thornes 1979, p. 262; Derbyshire et al. 1979, p. 54).

It is thus a natural law that the rate of soil removal - climatic, soil, land management and vegetative conditions remaining equal - increases with slope steepness and slope length. The steeper a slope is, the more rapidly will the surface water flow downslope. The high runoff velocity leaves the flowing water relatively little time to be absorbed by the soil, so that steeper slopes are also associated with a greater runoff volume, a factor of importance for total carrying capacity (Wischmeier and Smith 1978, p. 15; Zachar 1982, pp. 281-282; Breburda 1983, p. 31). As a rule, the same water collection effect is provoked by increasing slope length (Wischmeier and Smith 1978, p. 14; Schwertmann 1982, p. 12; Breburda 1983, p. 32). Deviations from this rule are possible only in the case of very little runoff, since in this case long slopes provide greater opportunity for the runoff to infiltrate, provided that the water infiltration capacity of the soil is sufficient (Toy 1977, p. 10).

In general, however, it is true that the severity of soil erosion caused by surface runoff increases with the steepness and length of the slope, since these result in greater runoff velocity and runoff volume.

Because the carrying capacity of flowing water increases proportinately to the 5th power of the runoff velocity, the mathematical relation between potential soil removal on the one hand and slope steepness and, although to a lesser extent, slope length on the other hand is exponential, not linear.

The first attempt to mathematically correlate these two relief parameters with soil erosion was undertaken by A. ZINGG (1940, cited in Kent Mitchell and Bubenzer 1980, pp. 18-20; Hudson 1981, pp. 196-198; Zachar 1982, p. 284) who carried out soil loss measurements on test plots with a range of different slope angles between 5 and 12%. His measurements revealed that soil erosion increases on average as the 1.49th power of the slope percentage:

$$E = f(S^{1.49})$$

where:

E = soil loss
S = slope percentage and the 0.6th power of the slope length:

$$E = f(L^{0.6})$$

where:

L = slope length
(see Fig. 5).

Fig. 4: Relation between soil erosion and the relief parameters of slope steepness and slope length.

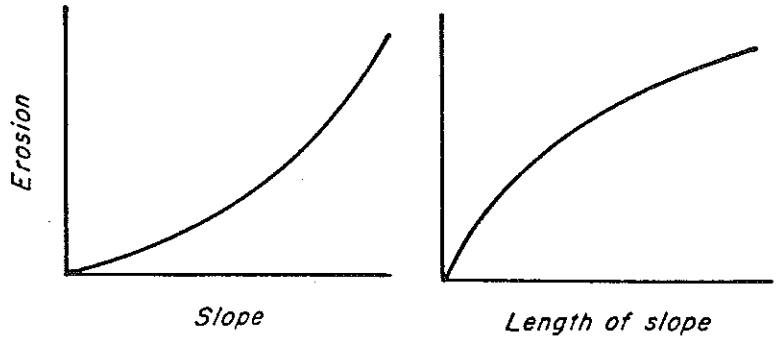

Source: Hudson (1981, p. 197)

From this it is evident that slope steepness has a far greater influence on soil erosion than slope length (see Fig. 4).

Other authors, like D. SMITH and W. WISCHMEIER (1957, cited in G. Richter 1965, p. 197 and Fig. 18; Hudson 1981, p. 196; Gehrenkemper 1981, p. 47; Zachar 1982, p. 284), improved the curves developed by A. ZINGG for slope steepness somewhat, and derived a slightly modified equation on the basis of the body of data available to them:

$$E = 0.43 + 0.30s + 0.043s^2$$

This yields a very similar curve, however (see Fig. 5).

Fig. 5: Soil loss as a function of slope sleepness on full (bare) fallow according to various American

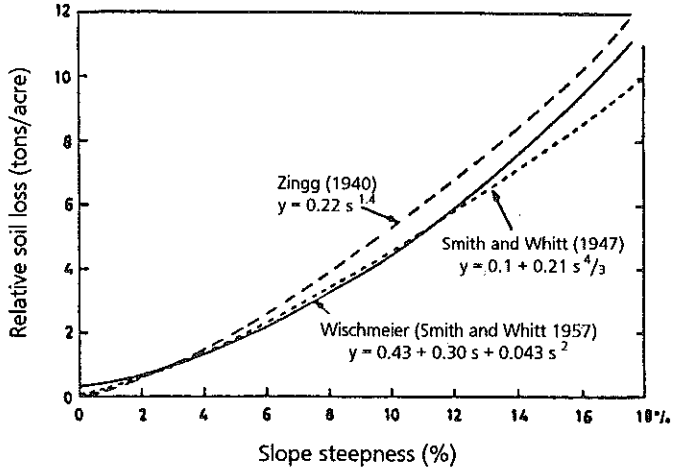

Source: G. Richter (1965, Fig. 18)

Studies conducted in the outer tropics, which are macroclimatically particularly endangered by erosion, have shown that under unfavorable conditions the influence of both slope steepness and slope length is even greater than in temperate latitudes. On soils with high erodibility and a sparse vegetal cover, soil erosion varies approx. as the square of the slope steepness:

$$E = f(S^2)$$

(Hudson 1977, p. 176; 1981, pp. 196-97; Roose 1977, p. 67).

The reference to soil erodibility and the protection afforded by plant cover provides an indication of the difficulty involved in quantifying the influence of relief independently of all other factors. The general rule that the effects of soil erosion increase exponentially with greater slope steepness and slope length only holds true when erosive surface runoff arises at all, which is usually only the case with structurally weak soils that are impermeable to water and bear a sparse vegetal cover (cf. Klaer and Krieter 1982, p. 156).

Besides relief, a central role is thus also played in soil erosion dynamics by vegetation, because the diverse ways in which it inhibits erosion have a stabilizing effect on the ecosystem (Toy 1977, p. 12; Morgan 1978, p. 9). The stabilizing function of vegetation, which has been clearly revealed by many studies (André and Anderson 1961, p. 3355; Strömquist and Johansson 1978, p. 48; Jung and Brechtel 1980, pp. 101-104; Gehrenkemper 1981, p. 46; Werner 1982, p. 109; Kaufmann 1982, pp. 213-214; Gerold 1983, pp. 6-7), is due to interception of the falling raindrops, increased infiltration, and reduced runoff velocity (as a result of increased surface roughness). In addition, both the root system and the surface biomass promote production of organic material and binding of the soil, important prerequisites for the formation of structurally stable soil aggregates with an improved infiltration capacity (Stocking and Elwell 1976, pp. 6-12; D. Moore 1982, pp. 37-38; Scheffer and Schachtschabel 1982, p. 421).

This makes it clear that the relief and vegetation are the factors with the greatest influence on the land and its environment, and thus also play a central role in connection with water erosion, which in the final analysis is a fundamental geoecosystemic process. It remains to be pointed out that the dynamics of soil erosion are primarily governed by relief if there is a lack of plant cover, while with the existence of a vegetal cover it is principally governed by the degree of coverage near the ground (Bergsma 1985, pp. 1-2). For example, soil erosion studies carried out in semiarid Kenya revealed that soil-loss rates drastically rose when cover density was less than a critical value of between 20 and 30% (Dunne et al. 1978, p. 136; cf. W. Richter 1971, p. 34).

A threshold value of comparable importance also appears to exist for slope steepness.

As can be seen in Fig. 5, at least up to a slope gradient of 18% (10°) there is an exponential relationship between slope steepness and soil loss. However, other studies have produced evidence to refute the assumption that soil loss rates continue to increase exponentially at greater slope angles, as the

connection discovered between slope steepness, runoff velocity and carrying capacity would lead one to expect and as is also postulated in the "slope topography nomograph" of the USLE for slope gradients up to just under 50% (26°) (Wischmeier and Smith 1978, p. 13; cf. ARBEITSGRUPPE BODENKUNDE 1982, p. 305).

For example, studies performed by H. HURNI (1985) in the highlands of Ethiopia and northern Thailand showed that an exponential relationship only existed between soil loss and slope steepness up to a threshold gradient of 24% (13°); thereafter the relation was linear. The cause of this gradient-dependent variance in soil removal dynamics could be the circumstance that less rain falls per unit area on steep slopes than on flatter slopes. This could have a direct influence on the runoff volume, a factor of importance for total carrying capacity (Hurni 1984, pp. 2 and 20).

The runoff model developed decades ago by R. HORTON (1936, cited in Weise et al. 1984, p. 33) also predicts that erosivity increases rapidly up to a slope gradient of 18% (10°), and then increases only very gradually in the gradient range between 18 and 36% (10-20°). When the upper limit is exceeded (36%), according to R. Horton's model soil erosion even decreases again. It should be kept in mind, however, that this model only incorporates runoff erosivity, for instance leaving the fact out of account that in the initial runoff zone, which according to the Horton model comprises a "belt of no runoff erosion", appreciable soil loss is often caused by the combined effect of impacting raindrops and the associated surface runoff (Cooke and Doornkamp 1974, pp. 32-34; Evan 1980, p. 115; Breburda 1983, pp. 45-46; cf. Thornes 1979, p. 264; 1980, pp. 131 and 162).

Nevertheless, the threshold values postulated in this classical model of relief-dependent soil erosion dynamics have been largely corroborated by more recent research results.

For example, soil erosion studies carried out by J. SCHWING and H. VOGT (1980, p. 213) in the Alsace region of France revealed that the various types of soil-erosion processes are most highly concentrated in the range of slope gradients between 20 and 36% (11-20°), i.e. within this range both sheet and channeled soil erosion are highly active. This finding fits in very neatly with the research results of C. WOODRUFF (1947, p. 477), who was able to demonstrate in experiments that the erosive power of surface runoff exceeds the erosivity of rainfall above a maximum critical slope gradient of 16% (9°).

J. SCHWING and H. VOGT (1980, p. 213) also identified a slope gradient of approx. 35% (19°) as the critical threshold for runoff erosion, similar to

that predicted by the Horton Model, but with the major difference that according to their results on even steeper slopes the further increase in overall erosion proceeds at a reduced rate, this being more or less distinct depending on the parent rock from which the soil was formed.

Comparable findings were made by F. GAZHIEV (1972, cited in Zachar 1982, pp. 282-284) in Azerbaijan in the Soviet Union. His field measurements revealed that soil loss increases most rapidly in the slope gradient class from 10 to 25° (18-47%), and that the rate of increase drops off again at even higher gradients (see Table 1).

Table 1 Soil loss as a function of slope steepness (based on field measurements in Azerbaijan, U.S.S.R.)

Slope gradient	10 - 15°	16 - 25°	26 - 30°	31 - 40°
Soil loss (t/ha)	61,4	148,5	195,0	240,5
Increase in soil loss (t/ha)	61,4	87,9	46,5	45,5

Source: Zachar (1982, p. 284)

If the above research results are reviewed in their entirety, it emerges that, as a function of relief, all possible water erosion processes can be expected to occur together on exposed slopes with gradients of between about 9-11° (16-20%) and 20-25° (36-47%), since within this gradient range not only erosion by impacting raindrops is active, but the surface runoff also reaches such a high degree of erosivity that, where soil erosion control is concerned, the further increase of natural erosion risk on even steeper slopes is negligible.

This gradient range is completely covered in the slope steepness map prepared in the course of this study, by the areas designated as medium slopes. A glance at the map also shows that almost all slopes in the selected study area belong to the class of the medium and steep slopes, which are - relief-induced - the most highly endangered by erosion.

5. The dynamic equilibrium between soil removal and formation of new soil

Worldwide, soil erosion represents the most important recent morphodynamic process affecting our planet's ecosystems. It was not until

soil erosion research was considerably intensified and extended to other parts of the world that the realization emerged, for many still surprising, that soil degradation is not just a phenomenon of unfavorable climatic zones; on the contrary, the agricultural landscapes of the temperate latitudes are for the most part also affected by severe soil erosion, although until recently little attention was paid to it because of its typically "creeping" character (Demek 1969, pp. 112-114 and 119-120; Grosse 1971, pp. 19-20; G. Richter 1980, p. 47; Leser 1977, p. 34; 1983a, p. 11; Breburda 1983, p. 5).

In order to conserve the soil as a renewable basic resource for agricultural food production, enormous global efforts are essential. In the long term, no more soil can be allowed to be lost than can be replaced by natural processes. Such a dynamic equilibrium is only possible if long-term average soil loss does not exceed certain site-specific tolerances, which primarily depend on the intensity of weathering of parent rock contributing to formation of new soil (G. Richter 1965, pp. 42 and 237). Expressed mathematically, the following conditions must be met:

$$W = T + D$$

where:

- W = formation of new soil by weathering, expressed as the depth in mm of newly formed soil (e.g. 10 mm/year)
- T = average soil loss in an area, expressed as the depth in mm of removed soil (e.g. 8 mm/year)
- D = lateral subterranean transport of material in solution, expressed as the depth in mm of soil (e.g. 2 mm/year)

and

$$T = W \times P_s$$

where:

- P_s = effective volume of the newly formed soil with progressive weathering (expressed as a dimensionless factor between 0 and 1) (e.g. 0.8)

The first equation means that formation of new soil from weathering of rock (e.g. 10 mm/year) must be at least as great as the total soil loss (e.g. 8 + 2

Fig. 6: The dynamic equilibrium between soil loss and soil formation by weathering

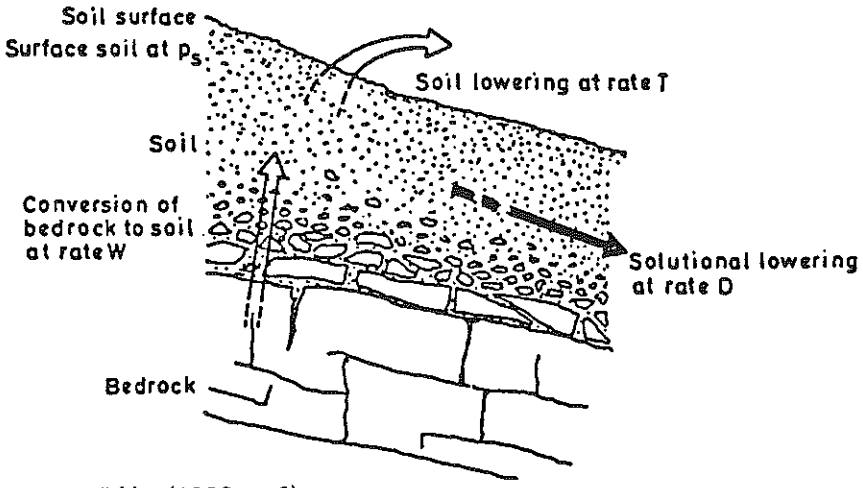

Source: Kirkby (1980, p. 6)

mm/year). The second equation means that surface lowering of the existing soil profile (e.g. 8 mm/year) must not be greater than the downward displacement of the soil-bedrock boundary as a result of weathering (e.g. 10 mm/year x 0.8) (Kirkby 1980, p. 6).

Because of the lateral transport of material which takes place in all geoecosystems, however, the conditions which must actually be met in order to maintain an equilibrium generally deviate somewhat from this ideal situation. In reality, *in situ* weathering is not the only important factor; the influx of soil and weathered material from sites situated at a higher elevation also plays a major role in maintaining the equilibrium between soil erosion and soil formation at a particular location (Heine 1978, p. 391).

A quite impressive example of this is provided by intact terrace complexes in former North Yemen, the fields of which are continually replenished by accumulation of weathered material washed in from above.

III. The situation in the Jabal Haraz area

1. Location of the study area

The GTZ project at which I worked in autumn of 1984 is located in the Jabal Haraz mountains, an isolated mountain massif roughly at the geographical center of the so-called "Serat mountain range" of former North Yemen. The project is based in the city of Manakhah (approx. 2,250 m above sea level; see Fig. 7), which was also chosen as the center of the field-study area (see maps).

Fig. 7: Location of study area.

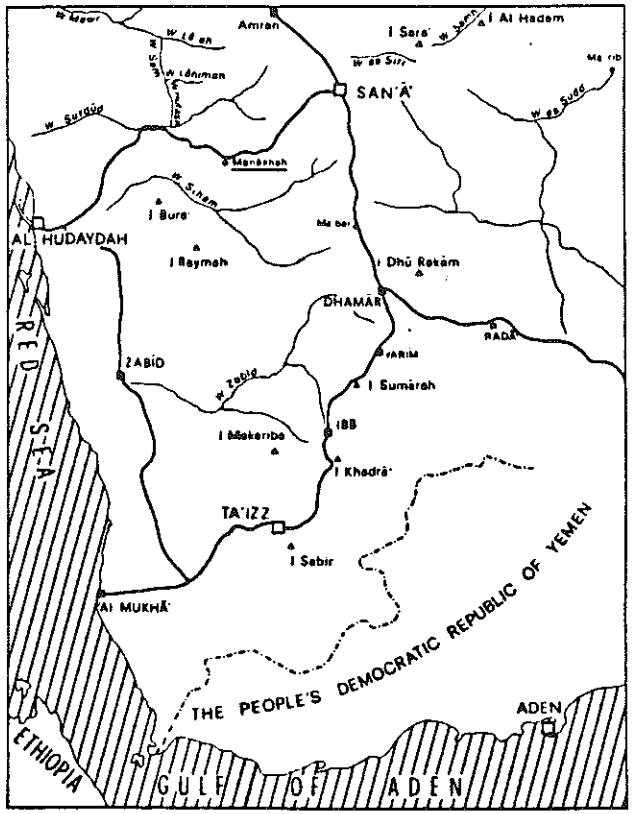

Comprising a total of 49 km^2, the study area was chosen in such a way as to maximize the likelihood of comprehensively surveying the complex of soil-erosion-related problems characteristic of this outer tropical mountainous region.

This meant that it had to be possible to study a large diversity of factors relevant to erosion. Prior to beginning the field work, maps and aerial photographs were evaluated, leaving no doubt that the relief has been the primary natural factor governing recent water erosion processes in this area. In order to permit study of as large a number as possible of different relief features (slope steepness, exposure, position, etc.) and relief-related parameters (precipitation patterns, agricultural techniques, etc.) the study area was defined so as to include the region's most important watershed area (Jabal Shibam at approx. 2,960 m above sea level) and, with the wadi extending from Jabal Shibam down to the tree nursery operated by the project (at approx. 1,350 m above sea level), a large portion of a major regional tributary water course (see maps).

The study area, the northern section of which is crossed by the Al Hudayda - Sanaa highway, is bounded by the geodetic coordinates 360,000 and 367,000 m E and 1,663,000 and 1,670,000 m N of the 1:50,000 topographical map of the Directorate of Overseas Surveys (1979), which is based on a transverse Mercator projection (see maps). These kilometer coordinates are approx. equivalent to the geographic coordinates 15°02′ to 15°06′ north latitude and 43°42′ to 43°46′ east longitude.

The maps used for this study - the map providing an overview of rock and soil samples (Map of Rock and Soil Samples), and the land-use and slope-steepness maps (Land-Use Map, Slope Steepness Map)- were prepared by photographically enlarging the topographical map from a scale of 1:50,000 to 1:10,000. Each of them was then traced on to a new topographic map, also on a scale of 1:10,000, with the 100-m isohypses missing on the original British map being added by interpolation. To improve their ease of use in this paper, the finished maps were then again reduced in size.

The kilometer coordinates used in the following for localization of important aspects refer to these maps, and were extracted from them using a chartometer which I devised myself.

2. Climate

a) The climate of former North Yemen

The mechanisms governing the climate of former North Yemen have not yet been satisfactorily explained, and a certain amount of contradictory information can therefore be found in the literature. While the nearby African Sahel is climatically characterized by a single rainy season during the summer, which can be quite adequately explained by migration of the "intertropical convergence zone" as a result of insolation, the highland regions of the Yemens - comparable to equatorial West and East Africa - exhibit a pattern of precipitation with two more or less prominent annual peaks, one reaching a maximum in the spring (April/May) and the other in the summer (July/August) (see Figs. 11 and 12; Rathjens et al. 1956, p. 10; Kopp 1981, pp. 44-46; Al-Hubaishi and Müller-Hohenstein 1984, pp. 27-28).

Since the sun reaches its highest point in the sky over the Yemens at these times, it would appear reasonable to regard both rainfall peaks as tropical zenithal rains (cf. Rathjens et al. 1956, pp. 9-10); these are known to be governed by migration of the intertropical convergence zone, which is tied to the equatorial trough, over the course of the year (Lauer and Frankenberg 1979, pp. 255-256). According to H. FLOHN (1965 p. 182), however, in Yemen these weather dynamics only apply to the summer rains, since the equatorial trough - and with it the intertropical convergence zone - does not reach its northernmost position at an average latitude of around 18 N until July/August. Consequently, at the latitude occupied by former North Yemen the southwesterly monsoon[3] winds of the summer months, which form part of the system of moisture-laden, structurally unstable equatorial westerlies, cannot converge with the stable and dry northeast trade winds in the lower troposphere until this time, thus creating the prerequisites for increased incidence of convective precipitation. In the southern portion of the Red Sea graben, the moisture-bringing air masses of the southwest monsoon rise towards this low-pressure area, burrowing "tunnel-like" into the upper tropical trade winds and attaining a vertical extension of up to 3 km (Flohn 1965, p. 190).

In contrast to these typical tropical summer rains, the "little rainy season" in the spring is ascribed by H. FLOHN (1965, p. 184) to the interaction of extratropical and tropical weather phenomena. In his view, the heavy spring

3) Originally from Arabic *mawsim* = season.

rains are related to both migratory high-altitude troughs in the extratropical westerly zone and expansion of the equatorial trough (Sudanese low) towards the north.

Penetration of such extratropical weather systems is permitted by the cellular structure of the subtropical high-pressure belt, and occurs primarily in the outer tropics as well as frequently in the highlands of equatorial East Africa (Lauer 1975, pp. 33-34; Lauer and Frankenberg 1979, p. 256).

Interpretation of the weather dynamics in this region is made even more difficult by the fact that the region around the gigantic Red Sea graben is orographically highly complex (Flohn 1965, p. 191). Here, planetary circulation is greatly modified both on a large scale (land-sea breeze cycle) and on a small scale (mountain and valley wind systems, air circulation on slopes). Due to the juxtaposition of extremes in insolation and relief, this outer tropical mountainous region has given rise to particularly intensive and expansive circulation systems which are characterized by large daily fluctuations in air pressure and have a decisive influence on the climate of the strongly dissected Serat mountain range (Flohn 1965, pp. 179 and 190).

For instance, a regular exchange of air masses takes place between the hot Red Sea basin (Tihamah) and the highland regions of the Yemen (Rathjens et al. 1956, pp. 17 and 28; Troll 1974, p. 211). During the day this takes the form of rising winds (a complex combination of offshore, valley and upslope winds) which are not only responsible for the frequent formation of fog on the slopes of the western escarpment, but here also serve to greatly amplify the effects of the planetary wind systems (Flohn 1965, pp. 179-180 and 190).

Another climatic phenomenon, which has also resisted efforts to definitively identify its causes, is that of the droughts which occur at irregular intervals and can last up to several years. Former North Yemen shares this phenomenon with the nearby African Sahel Zone, where - at least in the Sahel regions stretching from Senegal to Sudan - these droughts are due to failure of the summer rains. It is conspicuous that in former North Yemen these dry periods occur at more or less the same time and - like in the Sahel - have already attained catastrophic severity several times during this century (see Fig. 8).

According to informants in the area around Sanaa, the worst droughts experienced during this century in North Yemen were approx. between the years of 1903 and 1909 (Betzler 1987), compared to between 1907 and 1915 in the Sahel (Brown and Eckholm 1977, p. 17), as well as in both regions during the 1940s and the period from about 1967 to 1973 (see Fig. 8;

Gerholm 1977, pp. 35 and 56-57; Kopp 1981, p. 42). The dry period occurring during the first half of the 1980s has also been shared by both regions, and it is important to note that at least where the last few, relatively dry years are concerned it is a documented fact that the spring rains, generally regarded as unreliable, have remained unaffected in the study area (cf. Alkämper et al. 1979, p. 27; Kopp 1981, p. 48). Only the summer rainy season, which is tied to the intertropical convergence zone, has failed to reach its normal intensity (see Table 2).

Fig. 8: Precipitation cycles in the West African Sahel.

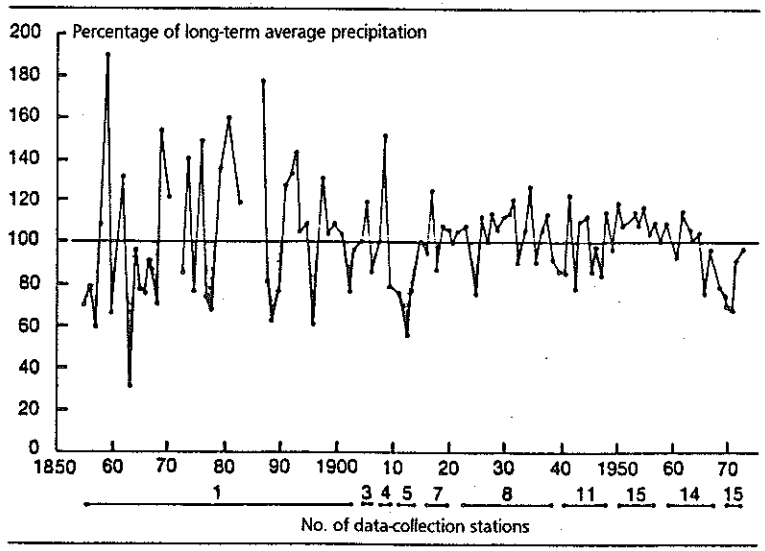

Source: Schädle (1982, p. 170)

The scant to completely absent summer rains are probably due to the influence of the dry northeast trade winds with their stable vertical structure, as has already been recognized by C. RATHJENS et al. (1965, pp. 9-10 and 15) for the Yemen highlands. This conclusion is also backed up by the results of research conducted in the neighboring African Sahel zone, which have shown that the main zone of precipitation is displaced by up to 200-300 km southwards by the humid monsoonal air mass carried by the trade wind (harmattan) (cf. Leroux 1983, 163-179). As earlier suggested by H. FLOHN (1963), the physical extent and intensity of this effect might at least partially be related to the nature and position of the upper current of the trade wind,

which during the northern summer develops into a quite constant jet stream with its core lying between 12 and 14° N (Besler 1981, p. 164), and which attains its greatest wind speed, of over 180 km/h, over southern Arabia in the month of August (Lockwood 1979, p. 117; Leroux 1983, p. 258).

This tropical easterly jet stream is characterized by upward movement of air masses on the southern flank of the jet core (main convection zone) and downward movement of air on its northern flank. According to H. FLOHN (1963, pp. 38-43) and H. BESLER (1981, p. 165), the downward movement on its northern side suppresses convection at the intertropical convergence zone, and is therefore the cause of both the abnormal summertime aridity of the entire dry belt north of the equator extending from the Sahara across Arabia and all the way to the Indus Valley, and of the periods of drought in the Sahel (Besler 1981, p. 163).

The most recent works, however, associate the periods of drought in the Sahel zone with anomalous changes in the surface temperature of the tropical seas which, as in the case of the El Nino phenomenon in the Pacific, in turn have a perceptible effect on atmospheric circulation (displacement of ITC towards the equator) (Lockwood 1986; Philander 1986). Initial data evaluations and pilot experiments suggest that the temporary drop in rainfall in the eastern Sahel zone (Sudan, northern Ethiopia), and in neighboring southern Arabia to the East, is primarily attributable to a complex interplay of oceanic/atmospheric circulatory disturbances in the region of the Indian Ocean (Palmer 1986).

b) The effective climatic conditions in the study area, illustrated with data from the Manakhah weather station

For description of the effective climatic conditions in the study area, in this section I concentrate on a discussion of data collected by the Manakhah weather station. Data on precipitation was gathered over a period of four and a half years, and can therefore be represented relatively meaningfully in climatic diagrams.

For the periods from December 1, 1982 to June 6 and June 23, 1985, for precipitation and temperature respectively, I had access to the weekly charts recorded by a pluviothermograph at a weather station owned and operated by the GTZ project. This was supplemented by data on precipitation collected in Manakhah by the YOMINCO (Yemen Oil and Minerals Company) during 1978 and 1979 and published by F. FASSBENDER (1982, appendix I, p. 1) in a project evaluation in the form of average monthly values.

In this particular case, the general problems posed by attempts to derive representative results from such brief observation periods were compounded by the fact that the evaluated data was not collected at a single site. From the beginning of 1982 until the beginning of May 1984 the project's weather station was situated on the roof of the Islamic School in Manakhah, at an elevation of approx. 2,300 m above sea level. Then, on May 5, 1984, it was moved to the roof of the local police station, which is at 2,250 m above sea level. It was not possible to determine where the YOMINCO weather station had been located.

The average daily temperatures were based on measurements taken at the so-called "Mannheim hours", namely 7:00 a.m., 2:00 p.m. and 9:00 p.m. The average daily values were calculated using the standard formula:

$$\frac{(\text{temp. at 7 a.m.}) + (\text{temp. at 2 p.m.}) + 2 \times (\text{temp. at 9 p.m.})}{4}$$

For calculation of the aperiodic daily amplitudes, the absolute daily minimum and maximum temperatures were also determined.

The evaluation of the precipitation and temperature data revealed that the Manakhah station is situated, climatologically speaking, in an outer tropical high-altitude zone characterized by a mild, seasonally moist climate. The outer tropical character of this site was evidenced, at an average annual temperature fluctuation of 7.3° C, by the temperature pattern, and due to the high variability of rainfall both from year to year and from season to season, and also by the rainfall regime. Between 44 and 86 precipitation events were registered per year (the frequent minimal amounts of moisture measured at 0.1 mm were most probably caused by heavy dew formation) (cf. Rathjens et al. 1956, pp. 5 and 7), and figures of between 340 and 570 mm were obtained for total annual precipitation. 1983 and 1984 were relatively dry compared to the significantly wetter years of 1978 and 1979 (see Table 2). The average annual rainfall figure of 471 mm for the entire observation period of four-and-a-half years is pleasingly consistent with the map of the average annual isohyets in this area published by J. KING et al. (1983, p. 80; see Fig. 9).

Fig. 9: Map of mean annual isohyets (mm).

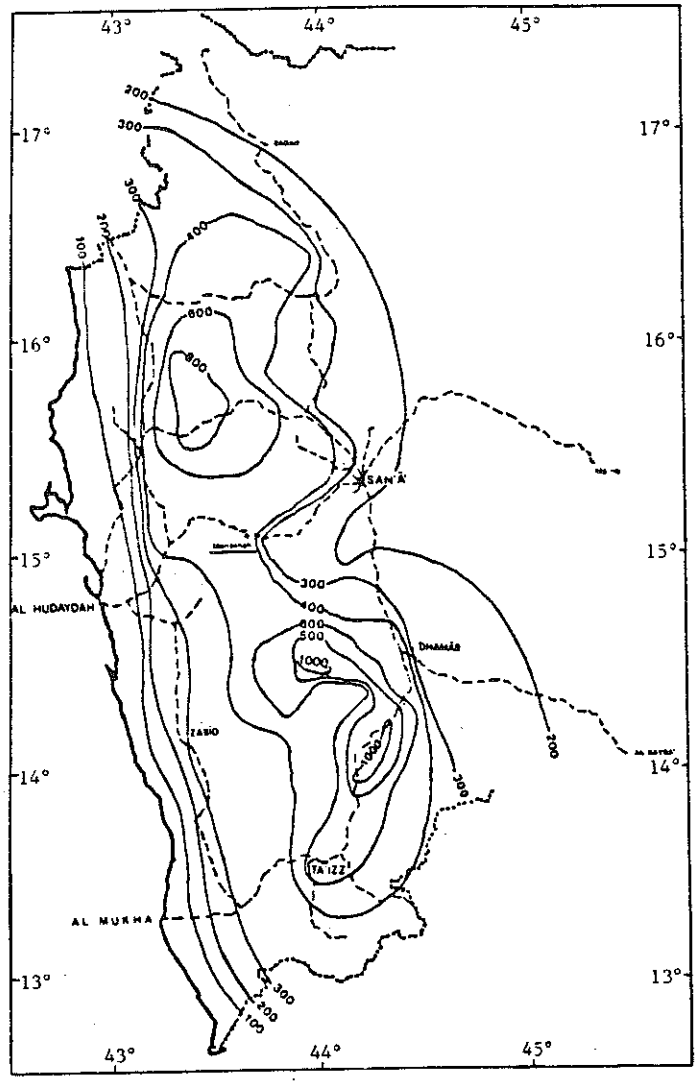

Source: King et al. (1983, p. 8) supplemented

My primary goal in evaluating the climatic data was not to arrive at a general climatic characterization of the region, however, but rather to gain a macroclimatic perspective on the site of the Manakhah station for

Table 2: Monthly distribution of precipitation (mm) recorded at Manakhah weather station

Year Month	1978	1979	1983	1984	1985	O
January	-	-	-	-	0.4	0.1
February	-	-	35.9	-	0.4	7.3
March	-	18.0	19.5	35.3	15.6	17.7
April	68.0	47.0	111.75	33.5	165.5	85.2
May	78.0	165.0	58.8	130.85	123.2	111.1
June	27.0	14.9	24.0	26.6	10.3[a]	20.6
July	153.6	88.0	35.25[a]	70.4		86.8
August	86.3	233.0	69.9	18.2		101.9
September	92.0	6.2	7.4	23.15		32.2
October	-	-	-	-		-
November	20.0	-	-	-		5.0
December	7.0	-	-	6.4		3.4
Total	531.9	572.1	362.2	344.4	(315.4)	471.3

a) partially extrapolated on the basis of data from the Ashami field

Source: GTZ Haraz Pilot Project (Manakhah station)
Fassbender (1982, appendix I, p. 1)

classification purposes. The principal criteria used for delimitation are presented in the following.

Situated at 15°04' north latitude, Manakhah is within the geodetic tropics, i.e. that portion of the globe in which the sun reaches its zenith (90°, or directly overhead) at least once a year, in which the declination of the sun's path relative to the horizon is never less than 43°, and at the boundaries of which (the Tropics of Capricorn and Cancer) it appears to reverse direction at the solstices (von Wissmann 1948, p. 81; Lauer 1975, p. 6). Because of the lack of seasonal extremes in the amount of solar radiation received, seasons characterized by prominent temperature differences occur only (to a very limited extent) towards the edges of the tropical belt. This uniformity of temperatures over the course of the year (annual isothermy), which can also be observed at all elevations above sea level in tropical mountain ranges, is typically coupled - due to the high position in the sky reached by the sun - with greater daily temperature fluctuations (Troll and Paffen 1964, p. 7).

C. TROLL (cited in Troll and Paffen 1964), who was the first to systematically demonstrate the existence of this pattern with the aid of thermoisopleth diagrams he developed himself, therefore refers to the tropical lowland and mountain climates as climates with daily periodicity (*Tageszeitenklimate*), as opposed to climates with seasonal periodicity. Moving towards the poles, the limits of such climates are generally reached where the annual temperature variance is 12° C or greater and/or the daily temperature variance (atmospheric temperature) is equal to annual temperature variance (Lauer 1975, pp. 17-19).

These limits roughly correspond to the Tropics of Capricorn and Cancer, i.e. the boundaries of the geodetic tropics. The same also applies to another tropical boundary, namely the limits of the warm tropics in terms of suitable climate for tropical vegetation and crops, identified by H. von WISSMANN (1948, pp. 86-87). These are formed by the absolute frost line in continental regions and by what von Wissmann calls the "lack-of-warmth line" (*Wärmemangelgrenze*) in oceanically influenced regions. The latter refers to the fact that the minimum warmth requirements of many tropical plants in oceanically influenced regions cease to be met not at the absolute frost line, but instead short of that point, in a threshold zone where the mean temperature of the coldest month drops to 18.3° C (von Wissmann 1966, p. 528; cf. Lauer 1975, p. 13; Lauer and Frankenberg 1977, p. 11).

This lack-of-warmth line, which is roughly equivalent to the limit of profitable coffee-growing, not only divides the maritime regions of the tropics from the subtropics, but also separates the tropical lowland climates (warm tropics) from the frost-prone montane climates (cool tropics) (von Wissmann 1948, pp. 86-88; cf. Lauer 1975, pp. 12-19). The existence of the latter was recognized in large part on the basis of observations made in Yemen by H. von WISSMANN (1948, loc. cit.), according to which the boundary zone between the "lack-of-warmth" line for coffee-growing and the absolute frost line, i.e. between the warm tropical "tierra templada" and the cold tropical "tierra fria", runs along the edge of the plateau at an elevation of about 2,200 m.

If the thermal criteria presented above are applied to the site of the Manakhah weather station, at an elevation of roughly 2,250-2,300 m, then it emerges - assuming, of course, that the brief observation period is representative - that we are dealing with a textbook example of a transitional warmth zone.

At a mean annual amplitude of 7.3° C and a mean aperiodic daily amplitude of 6.7° C, the station is situated in an outer tropical high-altitude region that

still exhibits prominent annual isothermy but does not fulfill TROLL's criterion for a climate with predominantly daily periodicity (daily temperature variance annual temperature variance). This interesting fact is certainly due to the frequent fogs and nocturnal flow of cold air downslope to lower elevations, thus preventing greater daily temperature fluctuations (cf. Rathjens et al. 1956, p. 26). In the final analysis, therefore, the lack of prominent daily periodicity in the climate at Manakhah is a consequence of the changing wind systems at different times of day - dissipating the heat at night that has accumulated during the daytime - which are in turn governed by the landscape relief (cf. Flohn 1965).

In hypsometric terms, Manakhah is situated - with a mean annual temperature of 16.6° C, a mean temperature of 12.7° C in the coldest month (January), and a coldest measured absolute temperature of 7° C (on January 15, 1985) - in a cool but frost-free altitudinal zone between the lack-of-warmth line and the frost line (von Wissmann 1948, p. 88; cf. Alkämper et al. 1979, p. 27), and therefore belongs to the cold, but oceanically influenced tropical "tierra fria" (see Fig. 10; Lauer 1975, pp. 17-19 and 24).

Fig. 10: North-south and altitudinal delimination of tropical zones on the basis of temperature criteria.

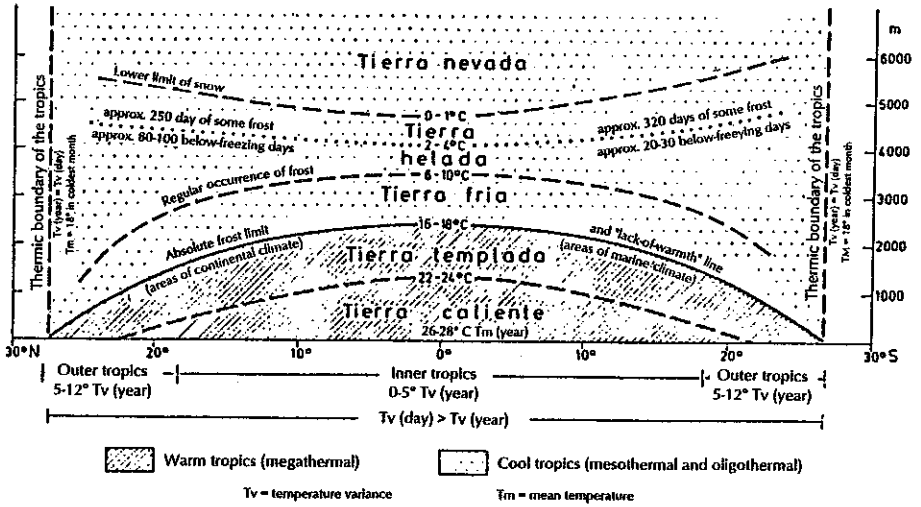

Source. Lauer (1975, p. 19)

The present-day extension of coffee-growing in the area around Manakhah provides a clear illustration of the broad transitional zone which H. von WISSMANN (1948, p. 88) identified at the lack-of-warmth line in Yemen. The coffee plantations extend towards the west up to an elevation of 2,000-2,050 m, and to the east, below Lakamat al Qadi, as far up as 2,350 m above sea level (see Land-Use Map). The transitional nature of Manakhah's climate is also demonstrated by the fact that qat-growing gradually comes to a halt at this altitude. Qat plants have minimum warmth requirements which cease to be met beyond the 17° C annual isotherm, at which frost becomes a latent threat (Revri 1983, pp. 19-20).

Due to the lack of seasonal periodicity of temperature fluctuations, the tropics are instead characterized by rainy and dry seasons of varying length and intensity.

Even when no measurement data on evapotranspiration is available, annual patterns of moisture and dryness can be easily calculated with the aid of empirical indices which, as a rule, are based on monthly temperature and precipitation. For the present study, the "index 20" of DE MARTONNE and LAUER (cited in Lauer 1951, p. 285) was applied. This computes the moist and dry months using the following formula:

$$\text{Index } 20 = \frac{12r}{t+10}$$

where:

r = mean monthly precipitation
t = mean monthly temperature

I decided to give preference to this index after reading a recent study by W. LAUER and P. FRANKENBERG (1981, p. 59), in which it was demonstrated, with the aid of a sufficiently well-founded evapotranspiration equation, that the threshold value of 20 in the old working formula for aridity was quite well-suited for identifying the dry months of the year, at least in the tropics. Accordingly, a month is regarded as dry or arid at an index of 20 or less, and as moist or humid at higher values. Data for compilation of a climatic diagram can be obtained by solving the equation for r or t (see Fig. 12).

In addition, with the aim of permitting comparisons of the climate at the Manakhah weather station with other sites in this and other regions (cf. e.g. Al-Hubaishi and Müller-Hohenstein 1984, p. 27), I also prepared a climatic diagram using the technique applied by H. WALTER (1973; 1979), who

published climatic diagrams for all of the earth's continents. With the aid of these diagrams, areas of similar or nearly identical climate (homoclimates) can be recognized at a glance (Walter et al. 1975).

This approach also compares temperature and precipitation for assessment of moist and dry months. The empirically derived yardstick of 10° C = 20 mm of rainfall (see Fig. 11) is applied. Months in which the average precipitation exceeds the numerical value for average temperature by more than a factor of 2 are regarded as moist, and all others as dry.

A comparison of these two methods shows that they reveal a consistent picture of the pluviothermic character of the Manakhah weather station site (see Figs. 11 and 12). In both diagrams, the moist phases of the spring and summer and the phenomenon of the "little dry season" in June are quite prominent. The same holds for the principal dry season lasting from September to March.

On average, therefore, four months can be classed as wet and eight as dry. In keeping with this overall pluviothermic picture, Manakhah can be treated as belonging to the semiarid cold tropics.

This general pluviothermic characterization could possibly require modification to take into account the undoubtedly occurring increase in climatic moisture as a result of fog formation on the exposed westward slopes.

For example, measurements taken using so-called fog-catchers (a pluviometer with an attached fog net developed by GRUNOW) at sites exposed to the wind within the zone of maximum condensation in Nepal yielded precipitation levels more than a third greater than those obtained from conventional measurements without a fog net (Haffner 1982, p. 7). Since the resulting increase in overall moisture goes hand in hand with greater edaphic (soil) moisture (Soil Survey Staff 1975, p. 52), information on the amount of fog condensation would be invaluable for analysis of ecological aspects.

Fig. 11: Climatic diagram acc. to the method by H. WALTER.

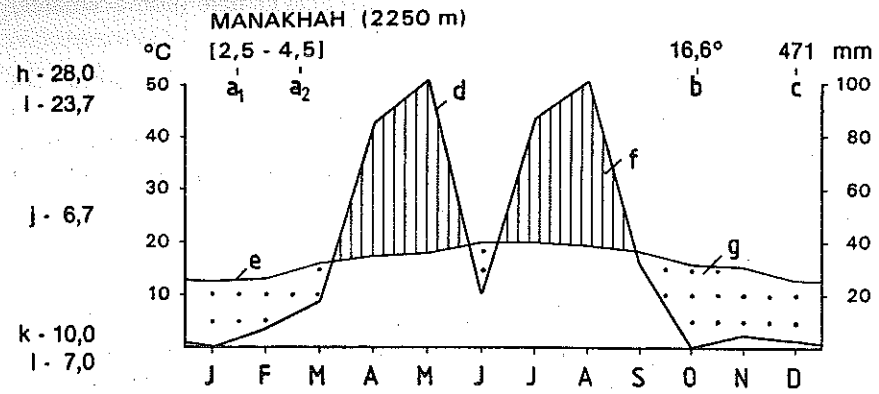

Design and artwork: H. Vogel (1985)

a1 = no. of years monitored (temperature)
a2 = no. of years monitored (precipitation)
b = average annual temperature
c = average annual precipitation
d = curve of average annual precipitation values
e = curve of average annual temperature values
f = relatively wet season
g = highest recorded temperature
h = highest recorded temperature
i = mean dialy maximum of warmest month
j = mean aperiodic daily amplitude
k = mean dialy minimum of coldest month
l = lowest recorded temperature

Fig. 12: Climatic diagram acc. to the method by E. DE MARTONNE and W. LAUER.

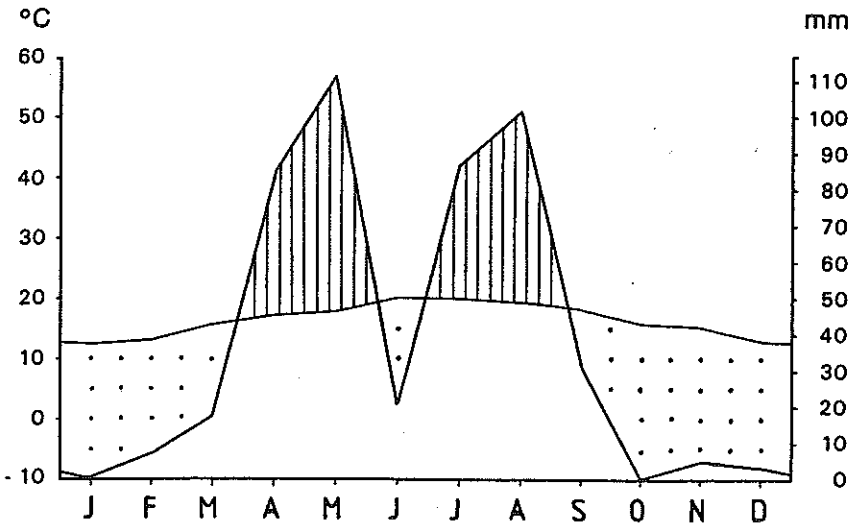

Design and artwork: H. Vogel (1985)

3. Geology

a) The tectonic-volcanic genesis of the Haraz mountains

The Haraz mountains consist of a steeply inclined horst which was uplifted by vertical block faulting in the course of formation of the Red Sea graben (von Wissmann et al. 1942, p. 271).

The block movements began with extensive horizontal movement (transcurrent faulting), which for the most part acted on predominantly meridionally aligned (north-south) zones of weakness of Precambrian origin (Bayer 1985, p. 162). This horizontal tectonic activity, the result of upward arching and crustal thinning of the Afro-Arabian Dome caused in turn by convective currents in the earth's mantle, led to continental break-up in the Eocene (Civetta et al. 1978, p. 309; Chiesa et al. 1983, pp. 642-643). While a segment of crust began to collapse at the crown of the greatly overextended

geanticline above the mound-like upwelling of the mantle, the areas adjacent to the emerging graben were simultaneously uplifted block-like by isostatic compensatory movements (cf. Bayer 1985, pp. 161 and 166). As lateral stretching of the crust proceeded, the downward displacements were increasingly accompanied by both explosive and extrusive fissural volcanism. This volcanic activity reached its peak in the Oligocene to Upper Miocene, when the upthrust graben flanks began to break up into smaller fracture zones (with formation of secondary grabens and horsts) (Geukens 1966, pp. B2 and B21; Civetta et al. 1978, p. 309).

During this time, sequences of fissure eruptions - for the most part of rhyolitic and basaltic lavas - and explosive ejection of volcanic ash (leading to tuff formation) gave rise to a Trap Series up to 2,000 m thick in the Haraz mountains. The viscous rhyolitic magmas also repeatedly provoked the explosive release of *nuées ardentes*, leading to formation of ignimbrites with differing degrees of welding (Civetta et al. 1978, p. 308).

In the case of the Red Sea graben this lateral pulling-apart of the earth's crust, which continues to this day (and is responsible for earthquakes and thermal springs), eventually led to the complete separation of Africa and the Arabian Peninsula (Martin 1985, p. 17). Since the Miocene, the original intracontinental graben has developed into a deep, wide rift which continues to grow as the Arabian Plate drifts towards the northeast at a rate of 0.7-1.1 cm/year (Bayer 1985, pp. 166 and 168).

b) The geological and lithological situation in the study area

In the Haraz massif the Tertiary Trap Series, also referred to as "Yemen volcanics" by M. GROLIER and W. OVERSTREET (1978), has a greatest age of 27 to 30 million years (originating in the Oligocene) as determined by potassium-argon dating, and attains a maximum thickness of approx. 2,000 m (Civetta et al. 1978, pp. 309-311; Chiesa et al. 1983, pp. 644-647). Its stratigraphic structure is characterized by an irregular sequence of alternating pyroclastic sheets and lava flows, as a rule ranging from 5 to 15 m thick.

Thin-section analyses of a total of 26 rock samples revealed the same lava lithotypes in the area around Jabal Shibam and Jabal Hudhar as S. CHIESA et al. (1983) had identified on the northern slope of Jabal Masar. The pyroclastic rocks around Jabal Shibam and Jabal Hudhar consist of ash tuffs and lapilli tuffs or lapillitic agglomerates. On the basis of their mineral composition, the lavas comprise an alkaline differentiation series grading from alkali basalt to hawaiite to mugearite to alkali trachyte, with a further

tendency to alkali rhyolite (cf. Trommsdorff and Dietrich 1982, pp. 59 and 73). The terms hawaiite and mugearite refer to rocks which are intermediate in composition and habit between basalt and andesite (cf. Aust 1985, p. 7) and can be distinguished on the basis of their somewhat modified magmatic differentiation. These porphyritic lava flows are characterized by a high ratio of plagioclase (soda-calcium feldspar) to ferromagnesian minerals (Chiesa et al. 1983, p. 647).

The area covered by the Yemen Trap Series is in reality a large basin inclined towards the Red Sea graben (Geukens 1966, p. B18; Chiesa et al. 1983, pp. 644-652). Accordingly, the Series slopes prominently downwards towards the west, for the most part with gradients of between 10 and 20 (see Map of Rock and Soil Samples; Aust 1985, pp. 7-8). In the Manakhah area, the concordant sequences of strata are repeatedly cut through by vertical bodies of intrusive basaltic rock in the form of dikes; these follow tectonic fault lines with a northeast-southwest strike direction (see Photograph 1; cf. Chiesa et al. 1983, p. 647). At some locations hydrothermal silicic acid solutions also circulated in larger cavities, leading to deposition of chalcedony (CH 11 on the Map of Rock and Soil Samples). The volcanic activity which formed the Trap Series was not continuous, being interrupted by quiet periods; this is evidenced by the existence of inter-Trap continental sedimentary deposits (Geukens 1966, p. B15; Civetta et al. 1978, p. 308; Chiesa et al. 1983, pp. 642 and 644). The fine-grained sandstone at the lower perimeter of the project's experimental plot (SD 22 on the Map of Rock and Soil Samples) is certainly an example of this phenomenon. Eruptions of highly fluid lava led to the formation of small plateaus in the study area. Where dark, basic volcanic rock strata of this kind have been laterally exposed, it is occasionally possible to observe the columnar jointing typically formed perpendicular to the direction of flow as a result of contraction during cooling. A beautiful example of such basaltic columns can be found on a high scarp of alkali basalt (BA 17) on the northern slope of Jabal Shibam (see Photograph 2).

Photo 1: Fine-grained, consolidated ash tuff (ET 1) and basaltic dike (DI 2) on Jabal Hudhar (seen here looking soith towards Jabal Shibam).

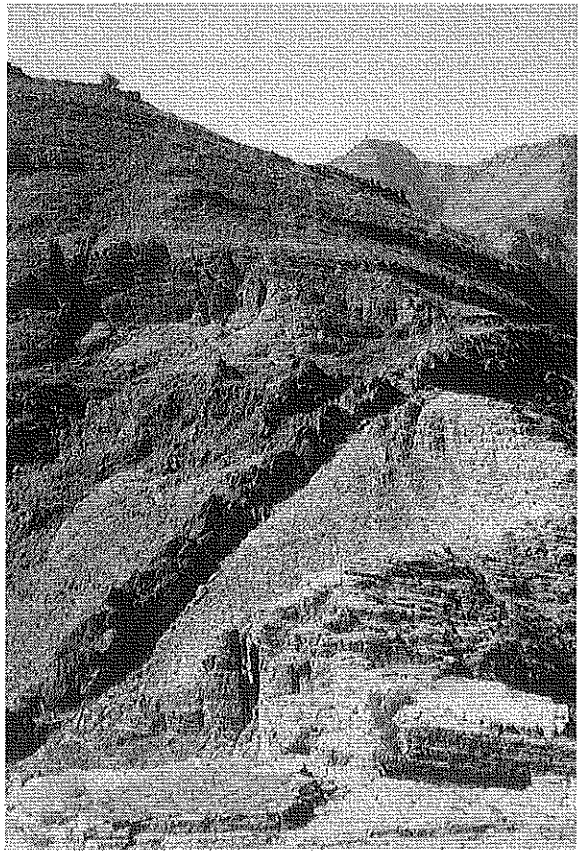

H. Vogel (9/25/84)

Photo 2: Columnar jointing in alkali basalt (BA 17) on Jabal Shibam (looking south).

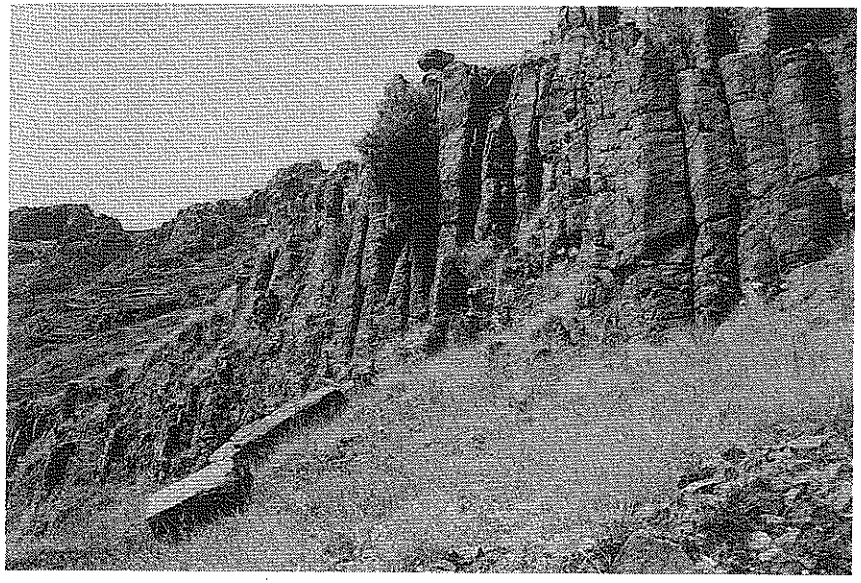

H. Vogel (9/6/84)

c) Thin-section analyses of various lithotypes on Jabal Shibam and Jabal Hudhar[4]

ET 1 - Ash tuff

Exceedingly fine-grained, highly consolidated green ash tuff containing a certain amount of metalliferous material, including limonite, which imparts a reddish color. With a chert-like appearance when its micrograph is regarded, this pyroclastite is bound together by altered glass (quartz), i.e. we are dealing here with formerly vitric tuff that cooled so rapidly after explosive ejection of the lava that mainly volcanic glass formed instead of crystals (cf. Dietrich and Skinner 1984, pp. 85-86 and 185).

4) The findings reported in this section are based primarily on analyses performed by Prof. Dr. J. Loeschke of the Institute for Geology and Paleontology of the University of Tübingen.

Map of Rock and Soil Samples

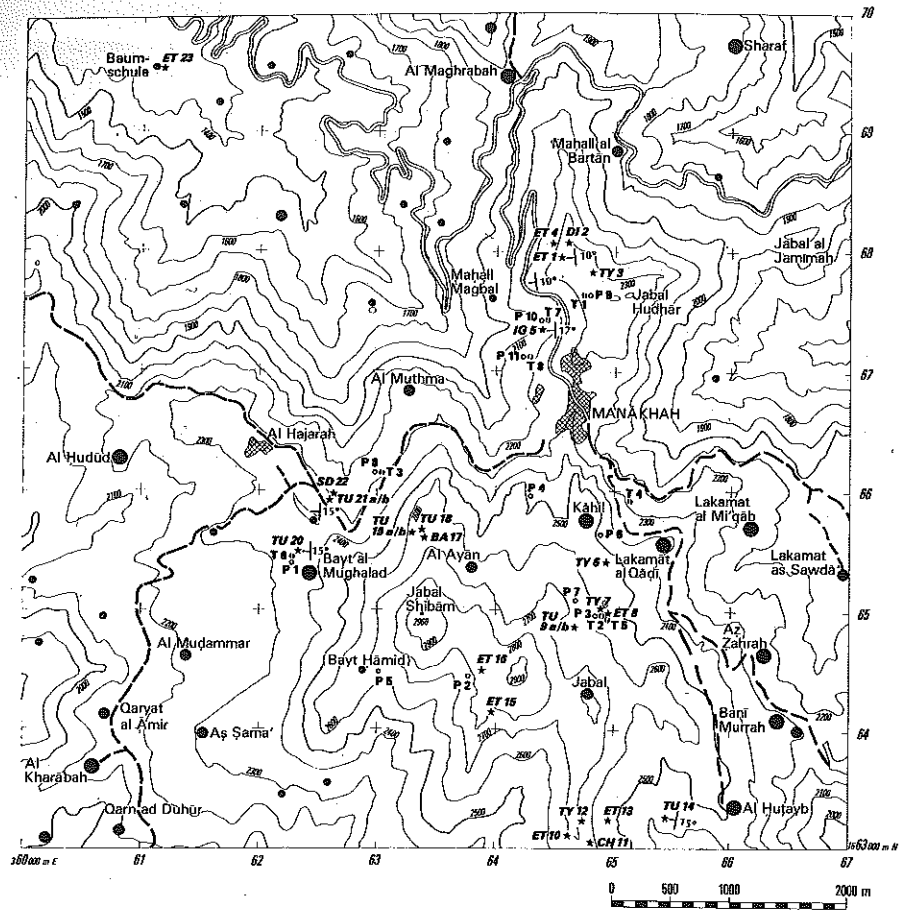

MANĀKHAH
Haraz Mountains

Soil samples:
Profile °
Terrace surface "
Rock specimens ⋆

Paved road
Unpaved road

Design and artwork: H. Vogel (1985)

Although S. CHIESA et al. (1983, p. 647) report partially to totally devitrified green peralkaline ignimbrites at Manakhah pass, microscopic examination of this sample revealed a fine-grained structure, but no deformed, collapsed and welded glass shards. Conceivably, this hand specimen was obtained by chance from an unwelded portion of the ash and pyroclast flow (cf. Trommsdorff and Dietrich 1982, pp. 111-112; Dietrich and Skinner 1984, pp. 201-202).

DI 2 - Basaltic dike rock

Intrusive basaltic rock from a dike, containing some apatite and large, partially carbonated phenocrysts of plagioclase, i.e. with a porphyritic texture.

TY 3 - Trachyte

Trachyte in which the feldspar has a conspicuous flow texture. Very high feldspar content, with large embedded crystals of sanidine (Carlsbad twins) and plagioclase, some quartz and metalliferous materials, and a few needles of apatite.

ET 4 - Trachyte

Lava with a very high feldspar content, a great deal of plagioclase, large potassium feldspars, some apatite and a certain amount of quartz, in a brownish-grey, dense groundmass. In this particular case, the quartz content of the rock indicates that it occupies an intermediate position between alkali trachyte and alkali rhyolite, although trachyte can also contain quartz (alkali quartz trachyte) (cf. Trommsdorff and Dietrich 1982, p. 81).

IG 5 - Ignimbrite

This rock is macroscopically very similar in appearance to the sample collected at ET 1, but when examined under the microscope the large number of welded and aligned glass shards showed it to be ignimbrite. The scattered pumice fragments are characterized by concave shapes. In addition to glass remnants, this rock also contains a number of potassium feldspar phenocrysts (probably sanidines) that, like volcanic glass, are highly susceptible to weathering. The red minerals occurring are hematite and limonite (formed by weathering of the hematite).

TY 6 - Trachyte

Porphyritic lava with partially carbonated plagioclase and a relatively large amount of metalliferous material. The groundmass contains fine-grained augites, and phenocrysts of augite also occur. A few brown biotites and their alteration product chlorite can also be discerned (alkali trachyte).

TY 7 - Trachyte

Trachyte with an attractive flow structure, some phenocrysts of carbonated plagioclase, and a small amount of quartz. The also discernible brown phenocrysts of titanobiotite are evidence of the alkaline differentiation series.

ET 8 - Hawaiite/mugearite

Basic lava with a wonderfully shaped porphyritic structure, a large number of plagioclastic phenocrysts, and much iron-bearing material (especially hematite, as well as a relatively great amount of limonite). The groundmass (matrix) also contains some fragmented glass and scattered acicular apatite. The mafic minerals - above all olivine, as well as a few pyroxenes - are fragmented. The high feldspar and iron-ore content and the low incidence of pyroxenes indicate that this is not a typical basalt; it is more likely hawaiite, or possibly mugearite. The high potassium levels measured in the soil (samples P 3, T 2 and T 5) favor the thesis that it is mugearite.

TU 9 a/b - Lapillitic agglomerate

a) Lapilli tuff (groundmass)

A very heterogeneous lapilli tuff containing basalt fragments rich in plagioclase and colored by iron-bearing minerals, as well as trachytic rock very rich in feldspars. Highly weathered, with the resulting gaps filled with calcite and clay minerals.

b) Bomb

This sample is a bomb (pyroclast ejected while viscous, receiving its rounded shape while in flight) formed from trachytic lava, containing many plagioclase minerals and some metalliferous material. The relatively great proportion of apatite is evidence of this rock's basically alkaline character. The dark constituents (olivine, pyroxene) are completely disintegrated (pseudomorphism). In addition, this rock contains some altered glass.

ET 10 - Mugearite

Porphyritic lava which is rich in plagioclase and metalliferous material, and contains some phenocrysts of potassium feldspar. Besides these large, prominently developed phenocrysts, apatites are also present in the matrix. In view of its mineral composition, this specimen is very likely mugearite (cf. Chiesa et al. 1983, p. 647; Trommsdorff and Dietrich 1982, p. 98). The partially discernible tendency towards a flow texture provides visible

evidence of the movement of the magma from which this rock formed (crystal mush).

CH 11 - Chalcedony

Fine quartz veins formed by hydrothermal deposition in cavities from water rich in silicic acid. Circulating water could have developed such a high SiO_2 content by dissolving the glass in rhyolitic lavas or acid tuffs (cf. Trommsdorff and Dietrich 1982, p. 111).

TY 12 - Trachyte

Trachytic lava with phenocrysts, some of sanidine and many of plagioclase, inset in a dense groundmass rich in feldspar and exhibiting a flow texture, i.e. the feldspars are arranged in a parallel pattern. Moreover, pseudomorphism by carbonation - giving rise to completely disintegrated pyroxenes - has taken place. The alkaline character of this lava is evidenced by its high apatite content.

ET 13 - Basalt/hawaiite

Lava of basaltic to hawaiitic composition and brecciated, i.e. consisting of an accumulation of angular fragments. It has a conspicuous porphyritic texture and isolated vesicular cavities. There are very large phenocrysts of plagioclase, some of which have been fragmented by mechanical stresses - probably during the flow stage - and others of which have been carbonated. The vesicles were created by escape and entrapment of gas and are filled with very fine-grained material.

TU 14 - Lapilli ash tuff

Coarse-grained, relatively heterogeneous pyroclastite with phenocrysts of plagioclase, a number of different potassium feldspars, and quartz. The isolated quartz crystals indicate that this is not a basaltic tuff. Iron-rich pigment minerals (limonite coatings) impart a violet hue to this rock, the predominantly ash matrix of which also contains lapilli.

ET 15 - Mugearite/trachyte

An intermediate differentiate composed almost entirely of feldspars (plagioclastic phenocrysts) and metalliferous pigment minerals, as well as a few apatites and disintegrated pyroxenes. Its texture is clearly porphyritic to fluidal in structure.

ET 16 - Hawaiite/mugearite

Porphyritic lava with plagioclastic phenocrysts arranged in a fluidal texture. The groundmass is also rich in plagioclase and metalliferous minerals. The relatively large proportion of metal-bearing minerals shows that this is not a genuine trachyte, and the lack of pyroxenes indicates that it is not a genuine basalt either. In actuality, this specimen is a rock intermediate in composition between hawaiite and mugearite.

BA 17 - Alkali basalt

Alkali basalt with a relatively coarse-grained groundmass, in which many plagioclase minerals and clinopyroxenes (titanaugites) occur, as well as apatites and metalliferous material. It also contains disintegrated glass and phenocrysts of plagioclase. There is clear evidence of pseudomorphism having taken place from calcite and possibly serpentine into mafic phenocrysts. The relatively high titanaugite content clearly demonstrates the alkaline character of this basalt (cf. Chiesa et al. 1983, p. 647; Trommsdorff and Dietrich 1982, p. 98). This specimen thus represents the primary rock of an alkaline differentiation series from which hawaiites, mugearites, alkali trachytes and alkali rhyolites were derived by further gravitational crystallization differentiation (cf. Trommsdorf and Dietrich 1982, p. 73).

TU 18 - Lapilli tuff

A very heterogeneous lapilli tuff containing crystals of plagioclase and apatite, characterized by a coarse-grained carbonated groundmass. It also contains a number of highly varied individual volcanic fragments.

TU 19a/b - Lapilli tuff agglomerate

a) Lapilli tuff (groundmass)

A lapilli tuff containing quite a lot of scoriaceous fragments of basaltic composition, some of which are extremely rich in vesicles and exhibit a porphyritic texture with phenocrysts of plagioclase. The vesicles (amygdules) are filled with a considerable amount of calcite, zeolites and a large number of other minerals.

b) Scoriaceous fragment

A porphyritic scoriaceous fragment characterized by carbonated megacrysts of plagioclase. The fine-grained groundmass contains crystals of plagioclase, olivine, clinopyroxene, some biotite, serpentine, and a relatively large quantity of iron ore (e.g. hematite, magnetite).

TU 20 - Tuff

A basic tuff with phenocrysts of plagioclase and variously colored fragments. The basic plagioclases are highly carbonated. The small vesicles which occur are greatly filled with carbonate which crystallized out of hydrothermal hydrogen carbonate solutions. Due to its high porosity, the fact that it consists largely of minerals that are readily weathered, and its relatively high carbonate content, it can be deduced that this specimen represents a very highly weathered tuff.

TU 21 a/b - Lapilli tuffs

a) Reddish lapilli tuff (upper part)

The material which binds this basic tuff together is slightly carbonaceous and high in clay. The many clay minerals present were produced by weathering of the volcanic ash. This tuff also contains remnants of "accretionary lapilli", which form by accretion of particles around wet nuclei, e.g. raindrops falling through a cloud of ash; in other words, this documents a subaerial eruption.

b) Light-colored lapilli tuff (lower part)

A tuff of basic composition cemented together by very highly carbonaceous material ($CaCO_3$ in cavities). This tuff also contains concavely shaped glass shards, highly vesicular pyroclasts (ash particles), metalliferous pigment minerals, and lapilli with phenocrysts of plagioclase.

SD 22 - Sandstone

Fine-grained sandstone very rich in quartz, set in a clayey matrix.

ET 23 - Rhyolitic ash tuff

This light-colored (leucocratic) ash tuff is characterized by a very fine-grained groundmass containing some potassium feldspar crystals and rock fragments.

d) The dynamics of weathering in the study area

When thin-section analyses and the observations made of the terrain are considered in their entirety, it emerges that a number of different, highly complex physical and chemical weathering processes are active in the study area. Due to the seasonally moist climate and the variable lithology of the study area, their effects fluctuate significantly in both time and space, as well as from lithotype to lithotype.

The physical weathering processes include hydration and salt weathering; the most important are those caused by insolation, i.e. variations in temperature. Chemical weathering is caused by oxidation and carbonation, as well as - above all - by silication, which is essentially a result of hydrolysis (cf. Alkämper et al. 1979, p. 29; Fassbender 1982, pp. 7-8).

Insolation weathering acts by inducing abrupt changes in temperature at the surface of rocks; in the study area, these are most liable to occur during the rainy season. The bright sunlight which falls during the morning hours greatly heats up the exposed rocks and minerals, especially the dark (mafic) ones. These expand and their crystal structure begins to fracture. If a rainstorm should then suddenly arrive during the afternoon the quenching action causes granular disintegration of the rock surfaces (cf. Wilhelmy 1981, p. 18; Schumacher 1983, p. 47). Evaluation of temperature data collected in the field revealed sudden atmospheric temperature drops of about 10° C during such events, with a subsequent rise of roughly 5° C.

Salt weathering probably also plays a role of some importance. As the thin-section analyses showed, calcium carbonate (calcite crystals) had often been precipitated out in rock cavities and microfissures. Because of its high coefficient of expansion and also because of the pressure exerted by it during the crystallization process, this calcium carbonate can be assumed to have contributed to rock fragmentation (cf. Schumacher 1983, pp. 48, 54 and 57).

Visible evidence of physical weathering can be observed in coarse-grained, porphyritic igneous rocks in the form of conspicuous surficial granular disintegration and scaling. By far the most spectacular symptoms of mechanical weathering are exhibited by highly porous tuffs, which literally crumble away. This can be clearly observed in terrace complexes where unstable pyroclastic rocks of this type have been used to build the retaining walls (e.g. specimens TU 20 and 21 a/b). The detritus resulting from such processes covers a particle size distribution ranging from heteroclastic blocks all the way to grit and silt.

In contrast to the coarse-grained lavas or even tuffs, the fine-grained extrusive rocks show few visual signs of mechanical or physical weathering other than crack formation. Some lavas (e.g. ET 10) exhibit strikingly spheroidal sheeting, although - comparable to the basalt columns - this most probably represents a primary type of jointing (cooling cracks) (Wilhelmy 1981, p. 13; cf. Press and Siever 1982, pp. 94-95).

Physical weathering of the fine-crystalline basaltic effusive rocks thus tends to advance quite slowly. On the other hand, microscopic examination shows these rocks to be highly prone to chemical weathering.

This is due, for one, to their chemical and mineralogical composition - characterized by readily weathered minerals (olivine, calcium-rich plagioclase, pyroxene, biotite and potassium feldspar) and glass of varying degrees of instability - and, for another, to their fine-grained structure (cf. Scheffer and Schachtschabel 1982, pp. 16-17; Press and Siever 1982, p. 91). The same also applies to the (highly porous) basic tuffs and highly vitric ignimbrites.

As is evident in the micrographs of the rock specimens, the unstable glass is usually quickly devitrified, being converted into zeolitic clay minerals, microcrystalline quartz and the like. Quite frequently, pseudomorphism by carbonation of calcium silicates (plagioclase, pyroxene) and of calcite-filled vesicles (amygdules) and joints is discernible. This observation is interesting, particularly as it relates to the calcium content of the soil; it provides evidence that $CaCO_3$ can even be derived from rocks originally lacking in carbonate, namely by combination of calcium cations (released from the primary minerals by hydrolitic weathering) with H_20 (rain, fog condensation) and CO_2 (from magma, the atmosphere or respiratory activity of microorganisms) (Ganssen 1965, p. 26; Jung 1965, p. 52; Jahn et al. 1983, p. 124; Schumacher 1983, pp. 48-49 and 53-54).

During the course of my field survey, I found only isolated instances of weathering caused by vegetation (by root action).

According to R. SCHUMACHER (1983, p. 54), microflora (algae, fungi, lichens) play an important part in accelerating the weathering of rocks and minerals, namely by biochemical and biomechanical action. Lower plants of this kind were also frequently observed in the study area, particularly on terrace walls on northern slopes and at relatively protected sites (see Photograph 19).

4. The relief

a) Morphology of the relief in the study area

The natural relief in the study area represents a typical trap landscape (von Wissmann et al. 1942, pp. 258-259). In spite of the strong superimposition of fluviatile erosion, the structure of the relief is essentially characterized by the varying morphology of the Trap Series, consisting of alternating, stratigraphically concordant sheets left by volcanic activity (cf. also Mensching 1982, pp. 42 and 46).

The most typical relief forms are plateau-like areas and stepped mountain and valley slopes. While the morphologically hard "trap basalts" and ignimbrites formed steep inclines and plateaus, the morphologically soft tuffs gave rise to slopes with intermediate gradients.

The overall structure and form of the relief are clearly illustrated by the pattern of the dense drainage networks formed by the periodically or episodically water-carrying dry river beds (wadis) and their tributary channels. This is most apparent in the mountainous relief of Jabal Shibam, where a radial network of wadis exhibits strong regressive erosion of the type that works its way upstream by undercutting action (cf. Map of Rock and Soil Samples). Thus, the upper courses of this system of valleys originating on Jabal Shibam possess a longitudinal profile with a very steep slope broken by vertical drops - outcrops and scarps of lava and ignimbrite - that form waterfalls when water is flowing in the wadis. Below the upper reaches where the steep stream lines abruptly turn into the otherwise flat floors of V-shaped valleys, outcropping lava sheets are deeply incised, ravine-like. Downstream from these abrupt breaks in flow line, the wadis are generally filled with rubble swept in from tributary channels. Where these tributaries tumble down the stepped valley slopes, this freight of rubble accumulates in fan-shaped to steep conical alluvial taluses, causing lateral displacement of the periodically or episodically flowing water and formation of even larger banks of rubble. As a result of this accumulation, which clearly is being aggravated by terrace abandonment, flooding of nearby farm plots and roads occasionally occurs in the peripheral zone of the study area; the Sanaa-Al Hudaydah highway has also been affected. The intensive erosive dissection of the mountain massif by these wadi systems, which drain to the west towards the Red Sea, is also apparent at the divide separating the drainage areas of the major valley systems of the Wadi Surdud (Wadi Shadhb) and the Wadi Siham (Wadi 'Ayyash). This already narrow divide runs south of Manakhah at an elevation of approx. 2,120 m above sea level (roughly following the course of the

unpaved road west of Al Hajarah) between Jabal Shibam (2,960 m) and Jabal Masar (2,760 m), and is being progressively dissected (see Map of Rock and Soil Samples).

In contrast to the radial wadi network originating from Jabal Shibam, the smaller subordinate catchment areas on valley and mountain slopes are characterized by dense, digitate to tree-like (dendritic) networks of channels.

The geomorphological significance of these drainage patterns has to do with their function as indicators of the relief-induced morphodynamics active in the area. Not only do they clearly indicate the type, direction and distribution of current geomorphological processes, but because of their great spatial density they also tell us about the high intensity of these processes, and thus about the extreme risk posed by water erosion in the mountain ecosystem of the study area (cf. Stocking 1972, p. 434; Morgan 1979, pp. 72-76).

b) The interaction of human occupation and the relief, and its implications for agriculture in the study area

In spite of its inhospitable relief form and relief dynamics, virtually all parts of the Haraz mountains were settled centuries ago. Terrace farming made it possible to agriculturally utilize this rugged mountain landscape, characterized as it is almost exclusively by medium and steep slopes (see Map of Slope Gradients).

As settlement of the area became denser, the natural relief was strongly influenced by human beings. By building many thousands of reinforced terraces and supplementary structures, human beings have created a domesticated landscape in this mountain region, adapting the natural geological trap structures of the relief and converting them into farming terraces (see Photograph 3). The natural trap landscape has been replaced by an anthropogenic terrace relief. For centuries, these "technogenous" small-scale forms have been the most widespread geomorphological feature in the study area, impressing their stamp on the relief. It was not until this century that droughts lasting several years at a time, combined with a changed political and socioeconomic situation, unleashed degradation processes (abandonment of settlements and farming land) on an extremely threatening scale (see Land-Use Map).

Photo 3: Terrace farming on Jabal Shibam (looking northeast toward upper Manakhah and Jabal Hudhar).

H. Vogel (11/3/84)

In view of what has been said so far, it is clear that the natural relief of the Haraz area - due to the extreme nature of its static and dynamic features - has had and continues to have an enormous influence on the processes involved in shaping the landscape and on human activities associated with use of the land (cf. Fig. 13; Kopp 1975, p. 65; 1981, pp. 97-111).

The relief of the study area is environmentally significant as regards its influence on the mesoclimate (wind systems with daily periodicity: fog formation, afternoon rainstorms, lack of significant temperature variations during the course of each day), the vegetation (hysometric variation), soil formation (lithomorphic soils, soil-water regime), surface runoff (dense drainage networks), and thus also the morphodynamics of water erosion (intensive dissection).

The functional significance of the relief for agricultural land use is the result both of the geoecological regulatory functions described above and of the direct influence which the static relief features - shape and size of the natural relief forms - have on agricultural techniques (terracing, rainwater harvesting,

anthropomorphic soils), the size and accessibility of farm plots (management methods), the choice of crops (agrogeographical altitudinal levels), and the yields and economic feasibility of land-use systems (subsistence farming predominates, with very little production of specific crops for marketing) (cf. also Kugler 1976, pp. 190-191; 1985, pp. 80-81).

Fig. 13: Functions of the relief.

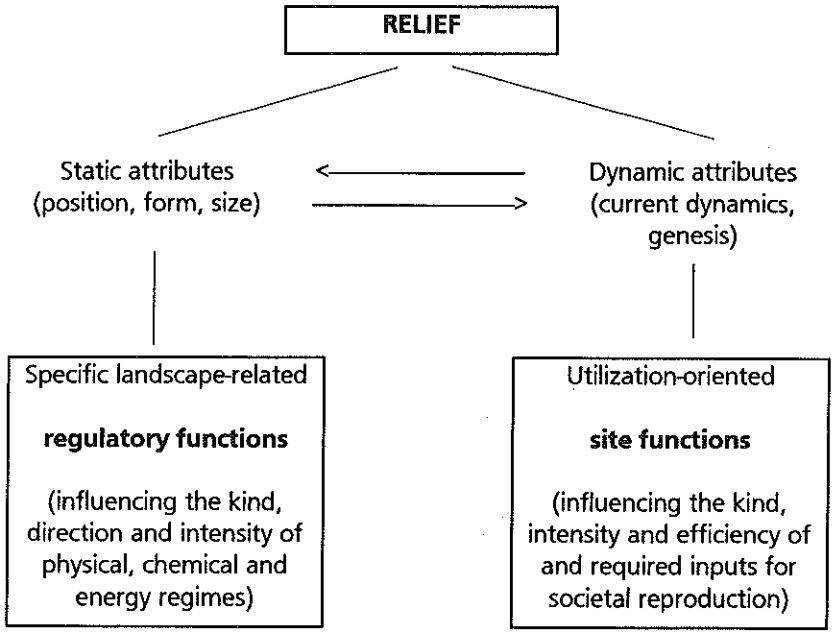

Source: Kugler (1977, p. 188)

If these relief factors are evaluated according to economic criteria and as regards farming techniques, it emerges that, without a doubt, the relief imposes narrow limits on agricultural production in the study area. The high population density and intensive agricultural land use in this mountainous region can only be explained as a child of necessity, in other words the inescapable need to exploit literally all available natural resources in order to feed a constantly growing population (Kopp 1985, pp. 44-45).

When general socioeconomic conditions change in such a way that this existential need to farm even the most marginal sites (i.e. plots that yield only just enough to ensure survival) vanishes, then it is only natural that the population will adjust to the new economic situation. Precisely this has happened in the study area, resulting in a fundamental shift in the value attached to the means of production.

Because of the availability of alternative employment (leading to emigration to neighboring oil-producing countries), former North Yemen's increasing integration into the global economy, and the considerable relief-related handicaps that must be overcome, the status of earning one's living from farming has drastically suffered in the Haraz area. Whereas previously the relative abundance of rain permitted (and limited) settlement and agricultural exploitation of this mountain area, now the relatively unfavorable relief (with the concomitant high labor and maintenance requirements, poor accessibility and limited possibilities for mechanization) is provoking a large-scale rural exodus.

5. The soils

a) Collection and test methodology

For the chemical and physical soil studies, mixed samples were collected of the topsoil (0-30 cm) and subsoil (30-60 cm) of 11 soil profiles, as well as from the uppermost surface horizon (the top 5 cm) of eight abandoned terrace sites.

The topsoil samples were collected at the standard depth for arable land (main rooting zone) (Kuntze et al. 1981, p. 257). The subsoil zone was defined following the example of F. FASSBENDER (1982, p. 9), who prepared a total of two project evaluations for the GTZ project in the study area. The decision to restrict this zone to between 30 and 60 cm below the surface instead of 30-100 cm (cf. Lenthe and Krone 1978, p. 24) was based on the fact that most wild and crop plants meet their water requirements primarily with moisture extracted down to approx. this depth (Späth 1975, p. 86).

The mixed samples of the soil profiles were taken in order to determine their erodibility (K factor) using the method described by W. WISCHMEIER et al. (1971) and W. WISCHMEIER and D. SMITH (1978), and for assessment of the economic potential of the soils. The surface samples (at each site, one from the base of the retaining wall and one from the edge of the field just in

front of it) were collected for the purpose of assessing the extent of sheet erosion at abandoned terrace sites.

Three of each sample were taken using a 100-cm^3 core sampler - for determination of bulk density (g/cm^3) - as well as along vertical strips in the profile using a spatula. The samples were dried in the project's oven in Manakhah for approx. 12 hours at 105° C, and subsequently passed through a sieve to eliminate soil fragments larger than 2 mm in diameter.

The soil analyses themselves were performed after my return from former North Yemen in the soil laboratory of the Geographical Institute of the University of Tübingen.

The soil profiles were surveyed in the field with the aid of a form based on a similar form published by S. MÜLLER (1969) but greatly modified to suit the requirements of this particular study and to take the special site conditions into account (see Appendix).

Color

Soil color was determined in the field with the aid of the MUNSELL soil color book (Munsell Color 1975), using moistened soil samples. When photographing the soil profiles, a color chart which I prepared myself, comprising 5 color fields, was photographed along with them; the purpose of this was to improve identification of the colors and compensate for distortion caused by differences in lighting, while providing a dimensional scale (10 x 30 cm) (Leser 1977, p. 22).

Particle size analysis

Each particle size analysis was carried out on 10 g of fine soil (i.e. with coarse fragments eliminated). After pretreating each sample with 10 ml of hydrogen peroxide (30% solution of H_2O_2) and dispersing it with 250 cm^3 of sodium pyrophosphate ($Na_4P_2O_7 \times 10\ H_2O$), a combined settling and wet-screening technique was applied.

The proportions of clay and silt were measured using analysis by the pipette method according to Köhn, with the sand fraction being subsequently recovered by pouring the soil suspension over a screen. In order to directly measure the very fine sand separate for determination of the soil erodibility (K factor), the standard set of sieves normally used in the Federal Republic of Germany for routine particle size analysis was supplemented by a fourth sieve with a mesh spacing of 0.125 mm. Consequently, the proportional weights of 8 instead of 7 separates (coarse, medium, fine and very fine sand, coarse, medium and fine silt, and clay) were directly measured.

A maximum margin of error of ± 3% was accepted. Only in a single case did it prove impossible to remain within this tolerance even after several repetitions of the analysis. The sample in question (T 2b) was thus entered with an error margin of ± 4.5%.

Carbonate

$CaCO_3$ content was measured using a SCHEIBLER apparatus with a 10% solution of hydrochloric acid (HCl) by gas volumetric analysis.

Soil pH

Soil pH was measured in each case by dispersion of 5 g of fine soil (i.e. without coarse fragments) in 20 ml of a 0.1-n KCl (potassium chloride) solution and electrometric determination (by glass electrode) with the aid of a DIGI 610 (pH 610 E) digital pH meter.

The measured values are possibly somewhat inaccurate, since the pH meter used exhibited a significant amount of drift over the course of time.

Phosphorus and potassium

Plant-available phosphorus and potassium were measured by weighing out exactly 5 g of soil and applying the CAL method by H. SCHÜLER. The P and K were extracted with calcium acetate lactate, and subsequently the normally indicated P_2O_5 content was determined by colorimetry using a PYE UNICAM SP6 - 500 spectral photometer for visible and ultraviolet/visible light. The K_2O (dipotassium oxide) content was then measured in ppm (mg per 1000 g of soil) by flame photometry using an Eppendorf flame photometer.

The nutrient contents cited in this paper are average values based on a minimum of two separate analyses. When the first two tests yielded contradictory results or implausibly high values, the samples were subjected to a third analysis and then the average of all three computed.

Organic matter (humus)

The amount of organic carbon in the soils was measured by reducing the samples to ash using the LICHTERFELDER wet incineration method (oxidation with potassium dichromate and sulfuric acid), determining the resulting chromium (III) ions by colorimetry (applying the technique developed by H. RIEHM and B. ULRICH), and multiplying by 1.724 to yield the organic matter (humus).

As in the test for phosphorus, colorimetric analysis was performed with the ultraviolet spectral photometer.

b) Classification of terrace soils

As a result of the extensive slope terracing, almost all the soils in the study area are agricultural soils. Soils in their natural state are rare.

Most of the artificially accumulated terrace soils are colluvia formed primarily by matter in suspension and larger by-products of weathering washed into the terrace fields by irrigation water from rainwater collection areas (*sawaqi* supplementary irrigation) or floodwater diverted from wadis (*sayl* irrigation) (Kopp 1977, pp. 24-25; 1981, p. 111; King et al. 1983, pp. 141-142). The parent materials are local volcanic rocks.

However, as I learned from questioning a group of farmers in the study area, the terraces are initially constructed by moving of material by hand according to an established schema. When creating new terraces, the first step is to pile up an initially low retaining wall or bank. Then the selected slope area is leveled by removing soil and weathered material from the uphill portion and dumping it on the downhill part (behind the wall). Occasionally, this is being supplemented by bringing in soil from elsewhere. In the third and last phase, a water delivery system is constructed and adapted to the size of the terraces. The actual filling-in of the terraces then usually takes place over a lengthy period of time, the soil being carried in with the irrigation water and accreting there as a consequence of the basin method of irrigation practiced in the area.

The alluvial terrace soils adjacent to wadi beds are built up according to exactly the same principle. However, these usually exhibit a much more pronounced fluvial stratification than the colluvial soils on the slopes (see Photograph 18).

The long-term sedimentation processes have caused soil formation to be repeatedly interrupted, so that lithologic-sedimentogenic features dominate in most soils and diagnostic horizons are generally poorly developed.

On the basis of their relative lack of distinct pedogenic horizons, within the soil taxonomy system of the U.S. Department of Agriculture (Soil Survey Staff 1975) the terrace soils belong to the order of the *Entisols*. Because they were formed by fluviatile and/or colluvial sedimentation, according to H.-R. LENTHE and F. KRONE (1978, pp. 23-24) they can be assigned to the suborder of the Fluvents, and their soil-water regime identifies them further

as belonging to the great group of the Torrifluvents (lat. *torridus* = dry). This classification was adopted by J. AIKÄMPER et al. (1979, p. 30) in their preliminary study on the Haraz project area, whereas F. FASSBENDER (1982; 1983) assigns the colluvial terrace soils in the study area to the suborder of the Orthents (soils that form on recent erosion surfaces and are either shallow to bedrock or contain more than 35% of coarse fragments), the great group of the Torriorthents and the subgroups of the Typic to Ustic Torriorthents (cf. King et al. 1983, p. 144).

In view of the fact that no data exists from long-term monitoring of the soil-moisture regime in the study area, however, it is not possible at this time to definitively assign these soils to great groups and subgroups of this classification system.

A well-suited soil taxonomy system to take the specific genesis of the terrace soils into account, in my opinion is the "morphogenetic classification system" developed by D. SCHROEDER (1984).

Within this classification scheme, the terrace soils correspond to *anthropomorphic soils* (cf. Asmaev 1968, p. 255), i.e. agricultural soils whose overall profile has been reshaped or created by human intervention. When such soils have been formed by manual deposition or artificially induced accretion, then they are aptly described as *Accusols* (artificially accumulated soils) (Schroeder 1984, p. 110).

Designation of the terrace soils as Accusols has the advantage that this term allows direct and unambiguous reference to their specific morphological features and anthropogenous formation (morphogenetic classification). The major disadvantage of this system is that it makes no provision for further differentiation of soils on the basis of textural or pedogenic attributes.

c) Characterization of the studied terrace soils

The unifying characteristic of most of the deep terrace soils is their relatively homogeneous basic structure; this is due to the predominant lack of pedogenetic (soil-forming) features. As can be expected in view of their formation by fluviatile and/or colluvial sedimentation, differentiation of their profiles is for the most part sedimentogenic in nature, a fact which is visually evidenced by the varying proportions of coarse fragments from layer to layer.

This relative homogeneity is clearly reflected by soil coloring. Based on the Munsell color charts, the studied soils exhibited, besides brownish-grey,

predominantly dark to very dark greyish-brown colors (when moist). There is only minimal vertical color differentiation (see Table 3; cf. Photographs 4 and 5).

Pedogenic processes are discernible in some profiles in the form of carbonate displacement and/or formation of a zone of *in-situ* bedrock weathering with clay formation and brownish coloring (cf. Fassbender 1982, pp. 7-8). While the carbonate processes have led to formation of fine, powdery calcium streaks, the development of a Bt horizon is evidenced in all 11 profiles by a slight increase in clay content as one moves downward from the topsoil to the subsoil (see Table 9).

Of interest are the increased percentages of clay in profiles 10 and 11, which are close to one another in terms of both location and site lithology (IG 5), and in profile 2 (see Map of Rock and Soil Samples; Table 9; Photographs 4 and 5). These profiles have higher clay contents than the other profiles, suggesting that more intensive autochthonous formation of clay minerals has taken place here from the readily weathered minerals present (mica, feldspars) and from unstable volcanic glass (cf. Jahn et al. 1983, p. 121; Schumacher 1983, p. 43). Also conspicuous is the high potassium content of profiles 10 and 11, which correlates not only with their high clay contents (= high capacity for binding potassium) but also, notably, with the mineral composition (potassium feldspar phenocrysts) of the parent rock (IG 5) characteristic of this site. Especially in the subsoil of profile 11, significant prismatic cracking has taken place of the kind that is typical of seasonally moist soil-water regimes in soils high in clay (caused by alternate swelling and contraction) (see Photograph 5). The high potassium levels in both the topsoil and the subsoil of this profile are likely due at least in part to their being transported downward by percolating water, since the 1- to 7-mm-wide dry cracks between the wedge-shaped soil blocks at the beginning of the rainy season provide ideal water channels (see Photograph 5). By the time the cracks have completely closed as the soil becomes saturated with water - which probably only occurs in exceedingly moist years because of the prevailing precipitation conditions (with long dry periods even during the rainy season) in the Manakhah area - significant amounts of water definitely manage to make their way down to considerable depths.

This penetration of moisture into the soil fulfills the prerequisites for activation of chemical weathering processes. Since the rainy season is during the warmer part of the year, this chemical weathering - above all in the form of hydrolysis - is additionally favored. On intact terraces these factors manifest

themselves in faster and more intensive soil formation than on unterraced sites (cf. King et al. 1983, p. 27).

However, since hydrolitic weathering is greatly accelerated by higher temperatures, greater moisture, and higher acidity (lower pH) of the soil, and none of these parameters attains particularly high levels in the study area, the absolute intensity of weathering in the soils is rather low. This expresses itself in dominant silt and sand fractions, as well as in an abundant supply of mineral nutrients. For example, the topsoils of the 11 studied profiles exhibited nutrient contents ranging between 30 and 350 ppm of P_2O_5 and between 80 and 420 ppm of K_2O. By Central European standards, these values range from low to extremely high (Kuntze et al. 1981, pp. 258-259; cf. Table 3). These nutrients are primarily of mineral origin, as can be deduced from a comparison of the results of the tests of the mixed soil samples and the findings of the thin-section analyses, in spite of the fact that the limited number of precisely corresponding rock and soil samples does not allow any absolutely definitive conclusions to be drawn. There is nevertheless an obvious correlation between the presence of potassium feldspars and apatite (calcium phosphate) in the bedrock on the one hand and higher soil potassium and phosphorus on the other (e.g. IG 5: P 10/11; T 7/8; TY 3: P 9/T 1). It should also be pointed out in this context that apatite, which is otherwise readily weathered (Schroeder 1984), is stable in neutral to slightly alkaline soils (see Table 3; Scheffer and Schachtschabel 1982, p. 241), but is dissolved by calcium acetate lactate, which was used as an extraction medium for analysis (Kuntze et al. 1981, pp. 257-258).

The same tendency can be observed with respect to soil calcium vs. the intensity of calcite formation in the rock (pseudomorphism by carbonation, and deposition in cavities) as established by the thin-section analyses. The complete correlation between the highest absolute $CaCO_3$ levels in rock (TU 20) and soil (P 1/T 6) samples taken from the "old trial plot" at Bayt al Mughalad is quite impressive.

The (low) calcium levels imparted to the soil by the parent rock (see Table 3) are apparently responsible for the extreme hardness which the terrace soils develop when dried out, as well as their generally high stability (stabilization of capillaries and cementation of primary particles). Thus, in a number of cases it was possible to observe streak-like calcium efflorescences along root channels and in soil pores, which provide evidence of downward carbonate migration. The upper limit of the calcium enrichment horizon is at a depth of between 30 and 35 cm, and this probably roughly corresponds to the average penetration depth of infiltrating water. By contrast, the lower

limit of calcium enrichment varies. In the five profiles containing prominent vertically aligned calcium streaks, the lower limit was at a depth of 55 cm in two cases (P 8 and P 9), while in the other three (P 3, P 6 and P 9) calcium streaks occurred over the entire excavated depth of 1 m.

At first glance it may appear a little confusing that in profiles 8 and 9 the calcium content of the topsoil was (somewhat) higher, in spite of the conspicuous calcium streaks in the subsoil (see Table 3). However, both were disturbed profiles on fields of the GTZ project on which soil excavated elsewhere had been spread during the course of the planting work. Since the other profiles studied also belong to abandoned terrace sites, the possibility that disturbances have also occurred there - particularly in the form of colluvial deposition - cannot be reliably excluded.

An extremely interesting soil-related topic which is discussed over and over again in the literature on Yemen has to do with the loess-like character of the terrace soils, posing the question as to whether eolian dust containing calcium, transported by the wind and redistributed by fluviatile action, has played a role in their formation (Kopp 1981, p. 41; King et al. 1983, pp. 19-20 and 26; Straub 1984, p. 204). The terrace soils do indeed exhibit a generally high proportion of silt (30-50%), a certain amount of calcium (0.5-9%) and high stability, adequate to high levels of plant-available nutrients, and - in spite of their general stoniness (10-50% of coarse fragments) - satisfactory to good water and field capacities (see Tables 3 and 9).

The extent to which these loess-like features can be attributed to the influx of eolian sediments redistributed by fluviatile action can, in the final analysis, only be guessed at. At least where the calcium content of the soils is concerned, the thin-section analyses make it seem plausible that the parent bedrock has also been the main source of carbonates (cf. Lenthe and Krone 1978, p. 25; Jahn et al. 1983, p. 124) and not windblown dust - or even Amran limestone lying beneath the Yemen Trap Series, which on the whole is roughly 2,000 m thick (cf. Kruck et al. 1984). As regards the silt fraction, only microscopic analyses could provide reliable information, since this is the only way to determine whether or not it is comprised predominantly of the same mineral spectrum which occurs in the volcanic bedrock - e.g. potassium feldspars and apatites. It should be pointed out here, however, that the granular structure of the fine-grained ash tuffs is similar to that of loess, and that the insolation weathering active in the study area is capable of disintegrating rocks down to the particle size range of silt.

Photo 4: Typical homogeneous soil profile structure on a terrace (P 2 on Jabal Shibam).

H. Vogel (8/28/84)

Photo 5: Terrace soil extremely high in clay, with characteristic cracking (P 11 near Manakhah).

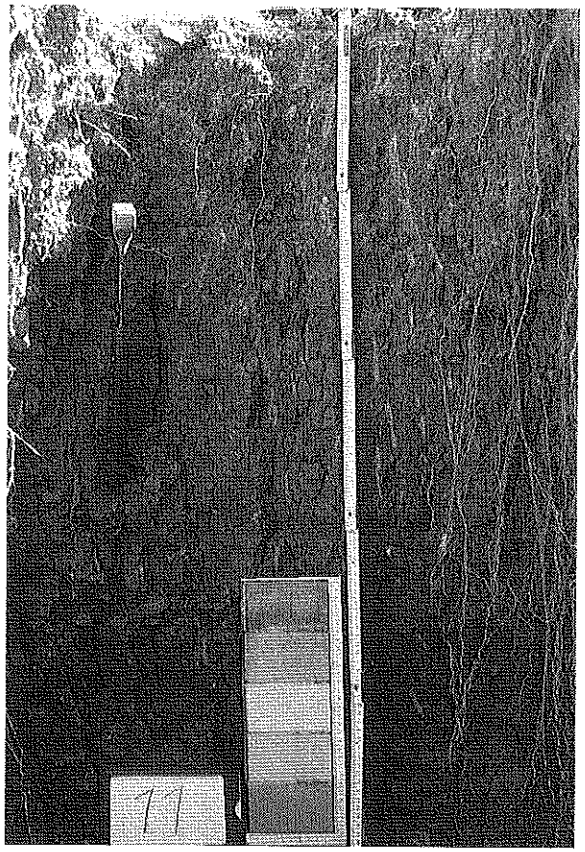

H. Vogel (11/6/84)

Table 3: Results of analysis of the investigated soil profiles.

No.	Site (map coordinates)	Lithotypes	Profile depth (cm)	Soil class	Coarse fragments (% vol.)	Soil color (when moist)	Bulk density (g/cm³)	Soil moisture (% weight)	nFK (mm)	pH (0,1n) (KC1)	$CaCo^2$ (%)	C	Humus (%)	P_2O_5 (ppm)	K_2O (ppm)
P 1	Bayt al Mugh. (62.30/65.40)	TU 20	0 - 30 30 - 60	loamy sand loamy sand	20 25	LOYR3/3	1.34 1.35	3.70 4.60	38 36	7.3 7.4	8.5 8.9	1.0 0.9	1.7 1.6	58 40	148 90
P 2	Jabal Shibam (63.70/64.40)	(ET 16 ET 15)[1]	0 - 30 30 - 60	loam loam	15 25	lOYR4/1 lOYR3/3	1.34 1.21	8.20 8.80	43 38	6.8 6.7	1.0 0.5	0.8 0.9	1.4 1.6	42 48	104 116
P 3	Kahil (64.85/64.95)	TY 7 ET 8	0 - 30 30 - 60	sandy loam sandy loam	10 15	lOYR4/3 lOYR4/3	1.40 1.42	- -	51 48	7.6 7.4	0.9 1.5	0.5 0.3	0.8 0.5	239 197	243 170
P 4	Westl. Kahil (64.20/65.95)	(TU 9a/b)[1]	0 - 35	silt loam	40	lOYR3/3	1.35	-	45	7.1	0.4	1.5	2.6	44	146
P 5	Bayt Hamid (62.90/64.55)	-	0 - 30 30 - 60	sandy loam loamy sand	25 30	lOYR4/3 lOYR4/3	1.38 1.45	5.75 5.91	43 34	7.4 7.4	0.5 0.8	0.8 0.4	1.3 0.6	216 104	298 148
P 6	East of Kahil (64.80/65.65)	(TY 6)[1]	0 - 30 30 - 60	loamy sand sandy loam	25 30	lOYR4/2 lOYR4/3	1.38 1.33	4.84 6.56	36 40	7.5 7.6	1.0 1.5	1.0 0.7	1.7 1.2	186 232	219 85
P 7	Above Kahil (64.65/65.10)	(TU 9a/b)[1]	0 - 30 30 - 60	silt loam sandy loam	40 50	lOYR4/3 lOYR3/3	1.30 1.30	- -	39 29	7.2 6.8	0.4 0.3	1.5 0.9	2.7 1.5	29 26	160 71
P 8	Ashami field (63.05/66.15)	-	0 - 30 30 - 60	sandy loam sandy loam	25 40	lOYR4/3 lOYR3/3	1.30 1.40	6.48 7.95	43 34	7.3 7.4	0.8 0.7	0.6 0.9	1.0 1.5	50 61	77 85
P 9	Manakhah (64.75/67.65)	TY 3	0 - 30 30 - 60	sandy loam sandy loam	50 10	lOYR4/2 lOYR4/2	1.40 1.40	12.68[2] 6.02	29 51	7.6 7.7	3.6 2.3	1.6 0.7	2.7 1.3	73 63	275 157
P 10	Manahkah (64.45/67.45)	IG 5	0 - 30 30 - 60	loam clay loam	25 35	lOYR4/3 lOYR4/3	1.27 1.43	7.00 9.70	38 29	7.6 7.6	1.5 1.7	0.7 0.5	1.3 0.8	152 55	385 168
P 11	Manakhah (64.25/67.10)	(IG 5)[1]	0 - 30 30 - 60	loam clay loam	20 20	lOYR4/2 lOYR4/2	1.38 1.59	6.22 11.35	41 29	7.7 7.7	3.3 4.5	0.7 0.4	1.2 0.6	352 92	424 415

1( ) = Certain rocks not from site

2 Rlt had rained the night before (11.1 mm recorded at Manakhah station on 9/9/84)

IV. Soil erosion in the study area

1. Socioeconomic background

During the last two to three decades, former North Yemen had experienced profound political and socioeconomic changes.

When the 7-year civil war came to an end in 1969, leaving North Yemen as a firmly consolidated republic, and the country opened itself to complete integration into the global economy, massive emigration of workers to the neighboring oil-producing states began (Kopp 1985, p. 46). Between 1970 and 1980 this manpower drain, provoked by the higher wages in the oil-producing countries, affected more than a third of the male population hitherto employed in agriculture, reducing its number from a previous level of 1 million to less than 700,000 (Steffen 1981, p. 73). During the same period, the number of Yemeni guest workers in the oil-producing countries of the Arabian peninsula - at an official population of 5,750,000 (1979/80) - rose from roughly 140,000 to 520,000 (Steffen 1981, pp. 75 and 79). Other sources place the number of North Yemenis working abroad on a short-term basis at that time at up to a million (Statistisches Bundesamt 1985, p. 28).

According to the census conducted in 1975, the Manakhah district has been affected more severely than most areas by this rural exodus. Thus, in 1975 the emigration rate[5] in the study area was 8%, i.e. at a total population of 34,919 persons (16,192 men) 3,036, corresponding to around 19% of the total and over 40% of the employable male population, were working in other countries (Steffen 1979, pp. 162 and 165-166). These figures have increased further since then, as is vividly illustrated by the abandonment and degradation of the village and fields of Bayt Hamid at the beginning of the 1980s (cf. maps).

As a result of the labor shortage which this development has caused in the agricultural sector, during the course of the 1970s the total farmed area in North Yemen was reduced by about 30%. The vast majority of the fields abandoned during this time were in mountainous areas like the Haraz, in which great effort had been put into terracing the slopes (cf. Land-Use Map). Grain-growing (sorghum, wheat, barley), which is for the most part

5) Emigration rate = individuals working abroad x 100 / total population + individuals working abroad